NASA
Technical
Paper
2674

1987

Material Characterization of Superplastically Formed Titanium (Ti-6Al-2Sn-4Zr-2Mo) Sheet

William A. Ossa
PRC Kentron, Inc.
Hampton, Virginia

Dick M. Royster
Langley Research Center
Hampton, Virginia

National Aeronautics
and Space Administration

**Scientific and Technical
Information Branch**

Identification of commercial products in this report is included only to adequately describe the equipment and does not constitute an official endorsement, either expressed or implied, of such products by the National Aeronautics and Space Administration.

Introduction

Research on advanced metals processing is being conducted at the Langley Research Center to develop improved forming and joining methods with the potential of reducing the weight and cost of future aerospace structures. Significant advances have been made in the processing of titanium alloys in recent years. Research studies have demonstrated that superplastic forming (SPF), superplastic forming/weld brazing (SPF/WB), and superplastic forming/diffusion bonding (SPF/DB) are viable processes for fabricating titanium structures which exhibit improved efficiency (refs. 1 and 2). The relative simplicity of the superplastic forming process alone promises to make a substantial impact on future structural components.

Recently, considerable interest in the aerospace industry has been focused on the near-alpha titanium alloy Ti-6Al-2Sn-4Zr-2Mo (Ti-6242). This alloy, with room-temperature mechanical and physical properties similar to the popular Ti-6Al-4V alloy, is being considered for use in high-temperature structural airframe applications because of its superior high-temperature (i.e., 1000°F) properties (ref. 3). Design criteria for these new applications make it paramount that high-temperature tensile and creep behavior be understood. The objective of the research reported herein was to characterize selected mechanical properties of Ti-6242 sheet in the superplastically formed condition, with and without subsequent heat treatment, and to compare the results with results of the same tests performed on as-received material, with and without heat treatment. SPF strains of 100 to 700 percent were investigated. Short-time tensile tests were performed at room temperature (RT), 600°F, 800°F, and 1000°F. Creep tests to 120 hours or 1-percent creep strain were conducted at 800°F and 1000°F. Finally, a metallurgical analysis was conducted to correlate tensile and creep data with changes in the microstructure caused by processing.

Materials, Equipment, and Procedures

Material Conditions

The mechanical properties of the Ti-6242 material were characterized in the as-received condition and in the superplastically strained condition, both with and without heat treatment. Tests were also conducted on material in an SPF simulated condition. These conditions are discussed subsequently. Table I presents the program test matrix and identifies the number of tests performed for each material condition.

As-received condition. Five heats of Ti-6242 alloy sheet were used in this program and covered a range in thickness from 0.015 to 0.090 inch. The material varied in silicon content from 0.05 to 0.08 weight percent and included sheet manufactured by three major titanium producers. Table II identifies the Ti-6242 heats used in this investigation and presents vendor-supplied information for each heat. Note that three of the heats were received in the mill-anneal condition, while the other two were in the duplex-anneal (mill-duplex) condition. The term "mill duplex" will be used in this paper to distinguish material in this latter condition from material which was duplex annealed during the program. Table III lists the chemical composition of each heat as reported by the vendor.

Superplastically strained condition. SPF material was obtained by axially straining sheets of Ti-6242 in the apparatus shown in figure 1. This apparatus would accommodate a panel up to 11 inches wide by 0.10 inch thick and would allow the panel to be strained to a final length of just over 16 inches. Optimum starting dimensions were determined for producing a strained panel with a predetermined amount of elongation to yield the maximum amount of material which could be used for property evaluation. Sheet material for these panels was sheared to size and chemically cleaned. The cleaning schedule used throughout this investigation included etching in a solution of nitric and hydrofluoric acids to assure a clean, uniform starting surface. Titanium 6Al-4V doublers were electron beam (EB) welded to both sides of each end of the sheet for attachment to the straining apparatus. The EB welds also changed the microstructure in the attachment area to the non-superplastic acicular alpha phase, which prevented this material from being inadvertently pulled into the strained zone. The panel configuration and components sized for a 400-percent SPF strain are shown in figure 2. After the panel was aligned in the straining apparatus, the chamber was evacuated to 10^{-5} torr and then brought to the desired temperature by using electrically heated elements. Temperature was controlled in the range of 1650°–1660°F and monitored with Type K thermocouples. A microprocessor-based process programmer with an MTS analog controller was used to maintain a constant strain rate during panel straining. After forming, the panel was permitted to cool to below 400°F prior to venting the apparatus to atmospheric pressure. Parameters for superplastically forming panels are listed in table IV. Figure 3 shows a 100-percent and a 700-percent SPF-strained panel, the minimum and maximum SPF strains used in the program.

A layout of each panel was made to document the location of metallographic and mechanical test specimens by identification number, as shown for panel 1 in figure 3(a).

Heat-treated condition. Although a variety of heat treatments have been developed for Ti-6242 material, the most common heat treatments for sheet are the duplex- and triplex-anneal conditions. The equipment used for heat treatment in this study included a large vacuum furnace capable of maintaining temperature within ±5°F, in a vacuum of 10^{-5} torr or better. Material to be heat treated was chemically cleaned as described previously and then suspended in the furnace by molybdenum wire to promote rapid heating and cooling during heat treatment. Thermocouples were placed between the parts to monitor the material temperature. The following heating and cooling schedules were used:

Duplex-anneal heat treatment:

1650°F, 1/4 hour; cool by forced He gas backfill
+ 1450°F, 1/4 hour; cool by forced He gas backfill

Triplex-anneal heat treatment:

1650°F, 1/4 hour; cool by forced He gas backfill
+ 1450°F, 1/4 hour; cool by forced He gas backfill
+ 1100°F, 8 hours

The first step in the heat treatment utilized an abbreviated alpha solution anneal (1650°F, 1/4 hour) because material thickness did not exceed 0.090 inch. Cooling was maintained at a moderately fast rate by forced inert gas backfill in order to approximate the cooling requirement of industry and military specifications (refs. 4 and 5). Recorded cooling rate was 375°F per minute from 1650°F to below 1000°F.

SPF simulated condition. The contribution of time at temperature on resultant properties of SPF material subjected to the thermal cycle to be encountered during forming was also investigated. Test specimens of as-received material were exposed to the same temperature-time cycle (without applied load) as 100-percent SPF strained or 700-percent SPF-strained panels as listed in table IV. These exposures, performed in a vacuum furnace, were terminated by moderately slow cooling to approximate the cooling rate experienced by SPF panels.

Test Specimen Preparation

Test coupons 3/4 inch wide by 8 inches long were sheared from as-received sheet in the rolling direction and from panels in the direction of loading unless otherwise noted. Coupons were cleaned prior to elevated-temperature exposure. The coupons were machined into test specimens, degreased, and again lightly etched to remove any residual contaminant. A single test specimen configuration (fig. 4) was used for all tensile and creep testing in this investigation. Rather than surface-grind test specimens to a uniform thickness, a thickness profile along the reduced section was determined for each specimen prior to mechanical testing. The cross-sectional area at the tapered end was used for calculating material properties. Metallographic specimens were sheared from sheet, strained panels (fig. 3(a)), and mechanical test specimens at the conclusion of the tensile or creep test.

Mechanical and Metallographic Test Procedures

Room-temperature tensile testing. Room-temperature tensile tests were conducted in a 10 000-pound-capacity screw-driven testing machine at a crosshead speed of 0.05 inch per minute through the yield point and then at the increased rate of 0.5 inch per minute to fracture. Load was recorded autographically against strain. Strain was measured by using polyimide-backed strain gauges bonded back-to-back on the specimen gauge length. Tensile strength, 0.2-percent-offset yield strength, and elongation in 2 inches were determined in accordance with ASTM E 8 (ref. 6). Modulus of elasticity was estimated from the initial slope of the load-strain curve.

Elevated-temperature tensile testing. Tensile testing to determine 600°F properties was conducted with the same equipment and at the same crosshead speeds as for the room-temperature tensile tests. High-temperature epoxy phenolic resin-backed strain gauges were bonded on each side of the midpoint of the specimen for these 600°F tensile tests. The specimen was heated in a resistance-heated forced-air circulating chamber mounted in the testing machine. Time to stabilize at temperature varied from 30 to 45 minutes. After being held at test temperature within ±5°F for 5 to 10 minutes, the specimen was loaded to failure. Tensile strength, 0.2-percent-offset yield strength, and elongation in 2 inches were determined in accordance with ASTM E 21 (ref. 7). Modulus of elasticity was estimated from the initial slope of the load-strain curve.

Tensile tests performed at 800°F and 1000°F were conducted in a 12 000-pound-capacity creep frame modified by replacing the crosshead with a motor-driven 4000-pound-capacity screw-type jack secured to the creep frame (fig. 5). Load was applied to the

specimen through the lower pull rod by the motor-driven jack and measured by a load cell placed in the load train between the specimen and the jack. Strain was measured by using a mechanical extensometer and a linear variable differential transformer (LVDT) shown in figures 5 and 6. The extensometer was centered on the specimen with the knife edges establishing the 2-inch gauge length. The assembly was then installed into the modified creep frame. Boron nitride was used as a lubricant/antiseize compound on the specimen grips and the extensometer. Strain rate through the yield point was controlled by selection of motor speed and gearing to obtain an initial measured rate of 0.006 per minute under load. After the yield point was reached, strain rate was increased by switching to a second motor. Type K thermocouples were wired to the specimen at the midpoint and just to the outside of the extensometer attachment points to monitor temperature across the gauge length. The hot junction of each thermocouple was placed between the specimen and a small titanium tab to shield it from direct radiation. New thermocouples were utilized for each specimen tested. Time to stabilize at temperature in the three-zone clamshell furnace was from 2 to 3 hours. Specimen temperature was controlled to within ±3°F for 30 minutes prior to load application and throughout the duration of the test. Load versus deflection in the 2-inch gauge length was recorded autographically. Tensile strength, 0.2-percent-offset yield strength, and elongation in 2 inches were determined in accordance with ASTM E 21 (ref. 7).

Creep testing. Creep tests were performed in air at 800°F and 1000°F over a range of initial stresses from 10 to 90 ksi in constant-load, 12 000-pound-capacity creep frames by using ASTM recommended practices (ref. 8). Creep was monitored by using the extensometer and LVDT arrangement described earlier. A programmable data logger with output recorded on paper tape was used to monitor the tests. The extensometer/LVDT combinations used in this investigation were calibrated over a range of 0.036 inch. The resolution ranged from 3.0×10^{-5} to 5.8×10^{-5} inch depending on the LVDT used. The extensometer was centered on the specimen with the knife edges establishing the 2-inch gauge length. The assembly was then installed into the creep frame. Boron nitride was used on the specimen grips and the extensometer as a lubricant/antiseize compound. Type K thermocouples were wired to the specimen at the midpoint and just to the outside of the extensometer attachment points to monitor temperature across the gauge length. The hot junction of each thermocouple was placed between the specimen and a small titanium tab to shield from direct radiation. New thermocouples were utilized for each specimen tested. Time to stabilize at temperature in the three-zone clamshell furnace was from 3 to 5 hours. Specimen temperature was controlled to within ±2°F for 30 minutes prior to load application. A temperature gradient within ±3°F over the specimen gauge length was maintained throughout the test by an automated temperature controller. The data logger was set to scan LVDT output every 6 seconds as the load was applied to the specimen. Zero time (time of full-load application to the specimen) was determined by visual sighting of the weights lifting off the weight pan. The data-logger scan interval was adjusted so that at least either 1 scan per 0.00005 strain or 1 scan per hour was obtained. Unless otherwise noted, the creep test was discontinued after 120 hours or 1-percent creep, whichever occurred first.

Metallographic investigation. The metallographic investigation was based upon microstructural examination of sections removed from specimens of as-received, SPF-strained, and SPF-simulation material, with and without subsequent duplex-anneal heat treatment. Standard metallographic procedures (ref. 9) were used for specimen preparation, with Kroll's reagent used as an etchant. The alpha plus beta grain size was determined by a line-intercept method, and volume fraction of primary alpha was determined by the point-count method (ref. 9). Transformed beta percent refers to the percent of the beta region which exists as transformed beta rather than metastable beta. Examinations were conducted with optical microscopy, scanning electron microscopy (SEM), and transmission electron microscopy (TEM). Energy dispersive X-ray analyses were used to support phase identification in the specimens.

Results and Discussion

Mechanical Property Results

Room-temperature tensile properties. Results of room-temperature tensile testing are tabulated in table V and typical trends are shown graphically in figure 7. Tests performed on material prior to SPF indicate the tensile data agree well with published data (ref. 10) for Ti-6242 sheet. The room-temperature tensile properties before and after various percentages of SPF strain are tabulated in table V and shown in the figure. A moderate drop in both tensile and 0.2-percent-yield strength is evident from figure 7. Post-forming duplex-anneal treatment did not restore properties to former levels.

The effect of SPF to strains of 700 percent on room-temperature properties shows further moderate reductions in tensile strength, yield strength, and elongation in figure 7. Curves are faired through the data. All three parameters show a trend of gradually decreasing properties with increasing SPF strains. Strength is reduced approximately 10 percent on the specimen which was 700-percent SPF strained and duplex annealed compared with mill-duplex material. Yield strength has dropped below 125 ksi on the same specimen; this is below the minimum yield strength requirement of specifications for Ti-6242 sheet (refs. 4 and 5). Room-temperature ductility, as measured by elongation in 2 inches, was also lower for large strains.

The results of room-temperature tensile testing on simulation specimens are also indicated in figure 7. The 100-percent SPF-simulation data points indicate only a minor change in properties from the duplex-anneal data points. However, the 700-percent SPF-simulation data points show a significant change in yield strength behavior. The yield strength of the 700-percent SPF-simulation specimen was similar to the yield strength of the 700-percent SPF-strain and duplex-anneal specimen. Examination of tensile strength and elongation results on these same specimens shows only a minor change in properties as a result of the 700-percent SPF-simulation cycle. The results of specimens which were duplex annealed after the 100-percent SPF-simulation cycle are also plotted in figure 7. No property differences were found between simulation specimens with and without subsequent duplex anneal.

Elevated-temperature tensile properties. Results of tensile testing at 600°F are tabulated in table VI, and representative trends are shown graphically in figure 8. The effects of various percentages of SPF strains to 700 percent are shown in plots of tensile strength, yield strength, and elongation against the amount of SPF strain. The tensile strength curves show that approximately 6 percent of parent material strength is lost after 100-percent SPF strain when compared with duplex-anneal material. Further reductions in tensile strength at increased strains were minor. The yield strength curves show that approximately 13 percent of parent material strength is lost after 100-percent SPF strain when compared with duplex-anneal material. Further reductions in yield strength at increased strains were also minor. Elongation, on the other hand, was not affected by the SPF process at strains less than 400 percent.

The results of 600°F tensile testing on simulation specimens are also indicated in figure 8. The tensile and yield strengths and elongations of 100-percent SPF-simulation specimens are nearly the same as the respective properties of 100-percent SPF-strained specimens. These data indicate that the thermal effect of exposure to 1650°F during the forming and subsequent quench rate is the primary reason for the decrease in the properties at 600°F observed in SPF material. Results of tests on specimens which were duplex annealed after the 100-percent SPF-simulation cycle are also plotted in figure 8. No property differences were found between simulation specimens with and without subsequent duplex anneal.

Tensile specimens were also tested at 800°F and 1000°F, with results listed in tables VII and VIII. Figure 9 summarizes graphically the effects of test temperature on superplastically formed Ti-6242 sheet. The figure includes data from the 125-percent SPF-strained and 200-percent SPF-strained panels. To remove the effect of thickness variation on properties, only specimens with a like thickness (0.015–0.017 inch) were reported in this figure. The plot indicates that superplastically formed material has moderately lower tensile properties and that 0.2-percent yield strength is affected more than tensile strength. Note, however, that the dashed and solid lines merge as temperatures approach 1000°F, indicating little or no loss in strength due to superplastic forming at this upper test temperature. Ductility was more variable and generally increased at temperatures above 600°F.

Creep properties. The creep behavior at 800°F and 1000°F was determined on sheet material before and after superplastic forming from 100 percent to 700 percent. Results of these tests are summarized in tables IX and X. Increasing the creep strength of Ti-6242 by silicon additions and solution treating high in the alpha-beta region has been well documented (ref. 11). The panels superplastically formed in this program displayed superior creep resistance compared with that of the as-received material, regardless of silicon content, and without a high-temperature solution anneal. To show the effect SPF processing has on creep behavior, creep curves for specimens from a single heat of material in the as-received, duplex-anneal, 100-percent SPF-strained, and 200-percent SPF-strained conditions are plotted in figure 10. For the same initial test conditions, 0.4-percent creep (the upper value observed for all tests shown) did not occur for more than 60 hours for 100-percent SPF-strained material but in less than 6 hours for duplex-anneal material. The panel strained 200 percent had an even higher resistance to creep, not reaching 0.4-percent creep strain

for 115 hours. Note that this improvement is apparent at creep strains as low as 0.1 percent but is less significant at the shorter test times. Note also that the silicon content of this heat is only 0.064 percent, which is below the 0.08 to 0.10 percent recommended for developing high creep resistance (ref. 10).

A Larson-Miller parameter plot for the time to attain 0.1-percent creep strain at constant temperature is shown for material without SPF in figure 11. The parameter is stated by the relationship $P = T(\log t + C)$, where T is temperature in degrees Rankine, t is time to the creep strain identified, and C is a curve-fitting constant ranging from 15 to 25 depending on the alloy. The value $C = 16$ is used throughout this report. Data obtained from as-received and duplex-annealed material are plotted along with curves from handbook data from reference 10. A review of the plotted data permits the following observations to be made. Mill-anneal material displayed a wide range in creep resistance. The Larson-Miller variation is related to heat-to-heat variation, with heat 2 generally displaying the highest creep resistance, whereas heat 3 displays the lowest creep resistance at any given stress level. This variation was expected because of the unspecified temperature range of this heat treatment; this resulted in greater latitude of mill practices. Also, mill-duplex and material duplex annealed in this study have similar 0.1-percent creep behavior. A single curve representing all five heats in both the mill-duplex and duplex-annealed conditions is faired through the data set and is repeated in subsequent figures. A third observation is that all data points for this combined data set fall below the curves for duplex-anneal sheet developed from handbook data. The results of these tests, however, are in close agreement with those recently reported for duplex-anneal material by Lockheed (ref. 12).

Whereas figure 10 indicates that superplastic forming enhances creep properties at a single temperature and initial stress combination, figure 12 shows that superplastically strained material has improved the 0.1-percent creep properties relative to material without SPF over the range of temperature and stress combinations investigated. The degree of enhancement is found to be stress dependent, decreasing as stress increases. Improvement in creep properties is attributed to grain growth which occurs during superplastic forming. Creep tests were also performed on SPF material after duplex annealing and triplex annealing. The results, plotted in figure 13, show a dramatic loss in creep resistance as a result of either heat treatment.

Time to 0.1-percent creep for 100-percent SPF-simulation specimens is plotted in figure 14. The properties of the simulation specimens are similar to those of superplastically formed material. The conclusion is that these properties are due to the thermal effects of the SPF cycle rather than the mechanical work of straining. The simulation cycle enhances creep properties of specimens, while the post-simulation duplex-anneal cycle reduces properties in a similar manner as was observed on superplastically formed plus duplex-anneal material.

Metallography Results and Discussion

As-received microstructure. Typical photomicrographs of longitudinal sections of the as-received Ti-6242 sheet material are shown in figure 15, and reveal a variation in grain size and microstructure from sheet to sheet. The three heats received in the mill-anneal condition are shown in the upper photographs, whereas the heats received in the duplex-anneal condition are shown in the lower photographs. Heat 3 is of equiaxed primary alpha (light) with islands of metastable beta at triple points and intergranular locations. This microstructure suggests a low-temperature anneal after rolling. Heat 2 shows equiaxed primary alpha (light) with transformed beta (dark) and a few islands of metastable beta, indicative of an annealing temperature closer to the beta transus of approximately 1815°F. As the annealing temperature is increased toward the beta transus, the volume fraction of primary alpha decreases, grain growth occurs, and metastable beta is replaced with transformed beta. The cooling rate also affects the volume fraction of primary alpha and is the reason for the rapid cooling requirement. The other as-received microstructures (heats 1, 4, and 5) show intermediate microstructures between these extremes. Note that even the microstructures of heats 4 and 5, both received in the duplex-anneal condition, are quite different. This degree of variation in microstructure was somewhat unexpected but permitted demonstration of the ease of processing by SPF for a wide variety of as-received microstructures. Heats 2 and 5 also show the beta phase to be somewhat elongated, indicative of rolling direction.

Table XI lists the volume fraction of primary alpha, percent transformed beta, and grain size by specimen code for all material conditions. The volume fraction of primary alpha in heat 2 is 77 percent, decidedly below the other heats; this also suggests a higher annealing temperature as mentioned. The relative amounts of beta and transformed beta varied considerably from heat to heat with the amount of transformed beta ranging from 0 to 70 percent of the beta region. No correlation was found between the amount of transformed beta in a specimen

and its tensile or creep strength. Grain size, on the other hand, was found to have a strong influence on creep resistance. Heat 2, which has a significantly larger grain size than heat 3, has much greater creep resistance, as indicated in figure 11. Heat 1, with intermediate grain size, was found to have creep resistance between heats 2 and 3. Even with this seemingly large heat-to-heat variation in the as-received microstructures, problems were not encountered in superplastic forming any of the heats.

Microstructure after heat treatment. The microstructures of heats 1, 3, and 5, after duplex annealing in vacuum as described in the experimental procedure, were examined and compared with those of the as-received material. Due to the relatively low (1650°F) annealing temperature and effectiveness of the cooling method, only minor differences in microstructure were observed. Table XI indicates an increased uniformity of the beta phase region and shows that two of the three heats had minor grain growth. The rather fine grain size of most of these heats in the as-received and the duplex-anneal conditions contributes to low creep resistance. This finding is the only one consistent with duplex-anneal creep properties lower than indicated by handbook data.

Microstructure after superplastic forming. Photomicrographs of specimens from several SPF panels are shown in figure 16 . Superplastically formed sheet has a microstructure which consists of an equiaxed primary alpha matrix with transformed beta (dark) and islands of metastable beta (outlined) at intergranular locations. This microstructure differs from the as-received structure primarily in grain shape and size and in proportion of beta regions which have transformed to alpha plus beta. The beta phase in the as-received material shows some directionality, but this is much less evident in SPF material. No evidence of direction of strain associated with the SPF process is noted. Although only one of the as-received and duplex-anneal specimens had a grain size above 4.9 microns, SPF specimens had grain sizes ranging from 5.2 to 7.0 microns for material strained to 400 percent. This increase in grain size, with attendant decrease in grain boundary volume (which acts as strengtheners at low temperatures), is the likely reason for the decrease in room- and elevated-temperature tensile strengths. The increase in grain size is also the only metallurgical observation supporting the improved creep properties of the superplastically formed Ti-6242 sheet. Note that most of the metastable beta has been replaced with transformed beta, which can be seen by comparing the SEM photomicrographs of figure 17. Formation of transformed beta in contrast to metastable beta in Ti-6242 is promoted by a lower concentration of beta formers (Mo) in the beta phase. A higher annealing temperature (such as 1750°F) coupled with rapid cooling will produce a microstructure which will be nearly free of metastable beta after the 1450°F stabilization treatment. In this investigation, such microstructures were developed as a result of SPF at the comparatively low temperature of 1650°F even though cooling rate was moderate (10°F/min). Although the reasons for this are not fully understood, both grain size and homogenization effects of the SPF process are thought to be significant.

No evidence of surface contamination, cavitation, or other defects was found as a result of superplastic forming during this investigation. Volume fraction of primary alpha remained approximately 83 percent. The primary microstructural variance found optically between various SPF panels was grain size, with the largest size found in the 700-percent strain panel. The relationship of grain size to time at temperature for Ti-6242 material is shown graphically in figure 18, with a plot of grain size against cumulative time at 1650°F. Grain size of the specimens which were not SPF strained is seen to follow the conventional grain size-log time relationship. In contrast, the grain size of superplastically formed material is seen to vary linearly with cumulative time at temperature. The grain growth observed in material SPF strained for short times is similar to the grain growth observed in similar heat treatment cycles. Note also that the 400-percent strained panel has a smaller grain size than the 300-percent strained panel as a result of the shorter time at temperature. In a design limited by creep behavior, it is conceivable that a lower SPF strain rate may be desirable to enhance creep properties.

Microstructure after mechanical testing. Figure 19 shows the microstructure of heat 3 in the conditions indicated. The only change from the SPF structure noted is that all metastable beta has transformed during creep testing. Equilibrium conditions for this alloy dictate such a small quantity of beta phase at use temperatures that most of the metastable beta will transform during elevated-temperature service. Confirmation of this was obtained by metallographic examination of various specimens of as-received sheet after creep exposure. In most cases, the metastable beta phase had transformed to alpha plus beta.

Microstructure after heat treatment of SPF material. Figure 20 shows the SPF microstructure of two panels in the before and after duplex-anneal conditions. This heat treatment has produced no obvious change

in the microstructure, which would explain the vast difference in creep properties. Grain size, which is known to influence creep properties, is essentially unchanged. For this reason, thin foil specimens of 100-percent SPF-strain panels before and after duplex anneal were prepared for TEM examination. Typical micrographs are shown in figures 21 and 22. Inasmuch as the primary alpha phase makes up at least 80 percent of these microstructures, this phase was examined first for evidence of substructure, particles, or subgrains to account for observed changes in creep properties. The TEM investigation also included examination of grain boundaries, dislocations, and transformed beta phase. Energy dispersive X-ray analyses were performed to support phase identification as indicated in the figures. No clear reason was found for the decrease in creep resistance found in superplastically formed sheet after duplex anneal.

Concluding Remarks

Considerable interest has been focused on the near-alpha titanium alloy Ti-6Al-2Sn-4Zr-2Mo (Ti-6242) because of both its high-temperature properties and its superplastic forming (SPF) capabilities. This paper describes current research to characterize selected mechanical properties of Ti-6242 sheet in the superplastically formed condition, both with and without heat treatment, and compares the results with those obtained on as-received material. The following remarks are based upon the findings of this study.

The as-received material properties of the sheet used in this investigation were found to vary considerably due partially to the mix of mill-anneal and (mill) duplex-anneal conditions. The tensile properties of superplastically formed Ti-6242 material are not the same as the published data base for Ti-6242 sheet. Room-temperature tensile strength, yield strength, and elongation all show the trend of slightly reduced properties with increasing superplastic forming strain and time at temperature. Approximately 10 percent of the parent material strength is lost after superplastic forming to 700 percent. Yield strength at 600°F was found to decrease approximately 13 percent. This loss in tensile properties was observed only at temperatures to 800°F. No difference in tensile properties was observed at 1000°F between as-received and SPF-strained materials. A post-forming duplex-anneal heat treatment has no beneficial effects on tensile properties.

Creep strength of Ti-6242 sheet is enhanced by the SPF process with the greatest improvement observed at 1000°F. An unexpected reduction in creep resistance of superplastically formed sheet was brought about by the duplex-anneal heat treatment. No differences in microstructure could be found by optical, scanning electron, and transmission electron microscopy to explain this reduction.

Properties of SPF material are affected by both the thermal effects of SPF, as well as by SPF strain. Room-temperature yield strength, creep resistance, and 600°F tensile and yield strengths change primarily as a result of the extended exposure at the SPF temperature. Decreases in room-temperature tensile strength and elongation at both room temperature and 600°F appear more related to total superplastic forming strain. Grain growth for Ti-6242 during SPF processing at 1650°F varies linearly with time.

NASA Langley Research Center
Hampton, Virginia 23665-5225
February 26, 1987

References

1. Bales, Thomas T., ed.: *SPF/DB Titanium Technology.* NASA CP-2160, 1980.
2. Royster, Dick M.; Bales, Thomas T.; and Wiant, H. Ross: Superplastic Forming/Weld-Brazing of Titanium Skin-Stiffened Compression Panels. *Materials Overview for 1982*, Volume 27 of *National SAMPE Symposium and Exhibition*, Soc. Advancement of Material & Process Engineering, 1982, pp. 569–582.
3. Taylor, Allan H.; Jackson, L. Robert; Cerro, Jeffrey A.; and Scotti, Stephen J.: Analytical Comparison of Two Wing Structures for Mach 5 Cruise Airplanes. *J. Aircr.*, vol. 21, no. 4, Apr. 1984, pp. 272–277.
4. Aerospace Material Specification: *Titanium Alloy Sheet, Strip, and Plate 6Al-2Sn-4Zr-2Mo Annealed.* AMS 4919A, Soc. of Automotive Engineers, Inc., Apr. 15, 1978. (Revised Apr. 1, 1984; Supersedes AMS 4919.)
5. *Military Specification - Titanium and Titanium Alloy, Sheet, Strip and Plate.* MIL-T-9046H (Interim Amendment 1(SH)), Jan. 21, 1981.
6. Standard Methods of Tension Testing of Metallic Materials. ASTM Designation: E 8-81. Part 10 of *1981 Annual Book of ASTM Standards*, c.1981, pp. 197–217.
7. Standard Recommended Practice for Elevated Temperature Tension Tests of Metallic Materials. ASTM Designation: E 21-79. Volume 03.01 of *1986 Annual Book of ASTM Standards*, c.1986, pp. 219–228.
8. Standard Recommended Practice for Conducting Creep, Creep-Rupture, and Stress-Rupture Tests of Metallic Materials. ASTM Designation: E 139-79. Part 10 of *1982 Annual Book of ASTM Standards*, c.1982, pp. 343–358.
9. Underwood, Ervin E.: Applications of Quantitative Metallography. *Metals Handbook, Volume 8—Metallography, Structures and Phase Diagrams*, 8th ed., Taylor Lyman, ed., American Soc. Metals, 1973, pp. 37–47.
10. Metals and Ceramics Information Center, Battelle Columbus Lab.: *Aerospace Structural Metals Handbook—1985 Publication*, Code 3718. (Formerly AFML-TR-68-115.)

11. Seagle, S. R.; Hall, G. S.; and Bomberger, H. B.: High Temperature Properties of Ti-6Al-2Sn-4Zr-2Mo-0.09Si. *Metals Eng. Q.*, vol. 15, no. 1, Feb. 1975, pp. 48–54.

12. Kaneko, Russell S.: *Ti-6Al-2Sn-4Zr-2Mo Structural Development.* NASA CR-166006, 1982.

Table I. Test Matrix for Characterization of Superplastically Formed Ti-6Al-2Sn-4Zr-2Mo Sheet

Specimen code (a)	Number of test specimens at —					
	RT tensile	600°F tensile	800°F tensile	1000°F tensile	800°F creep	1000°F creep
1M(0)-N					1	1
2M(0)-N	2	2				2
3M(0)-N	6	6			3	3
4D(0)-N	2					2
5D(0)-N	2	2			4	3
1M(0)-D	2	2	1	1	2	2
3M(0)-D	4	4			2	3
5D(0)-D	2	2			2	3
3F(100)-N	6	5			2	2
2F(125)-N	2	1	1	1	2	3
3F(200)-N	2	2	1	1	2	3
4F(200)-N	2	2			2	3
5F(400)-N	2	2			1	2
3F(100)-D	4	4			2	3
5F(300)-D	1				1	1
5F(700)-D	1	1			1	1
3F(100)-T					2	2
3S(100)-N		1			1	
5S(100)-N	2					2
5S(700)-N	2					
3S(100)-D		2			2	
5S(100)-D	2					2

[a] Example of specimen code:

3	F	(100)	-	D	2
(1)	(2)	(3)		(4)	(5)

(1) Heat code (see table II): 1 through 5.
(2) Condition: M, mill anneal; D, duplex by mill; F, formed; S, simulated.
(3) Percent strain (actual or simulated elongation): 0 through 700.
(4) Pretest heat treatment: N, none; D, duplex; T, triplex.
(5) Specimen differentiation: 1 through 6.

Table II. Titanium Sheet Thicknesses and Identification

Heat code	Heat	Thickness, in.	Condition (a)	Specification (a)
1	890808	0.015–0.017	Mill anneal	Mil-T-9046H
2	890414	0.022–0.024	Mill anneal	Mil-T-9046F
3	905387	0.032–0.033	Mill anneal	Mil-T-9046H
4	P6854	0.063–0.065	Duplex anneal	AMS 4919
5	S2203	0.088–0.091	Duplex anneal	AMS 4919

[a]Vendor-supplied information.

Table III. Chemical Composition of Titanium Sheet Material

Heat code	Chemical composition, weight percent (a)											
	Al	Sn	Zr	Mo	Si	C	N	Fe	O	H	Y	Ti
1	6.13	2.00	3.92	2.15	0.05	0.02	0.008	0.04	0.119	0.0102	0.0006	Balance
2	6.05	1.94	3.80	2.00	.06	.02	.011	.04	.13		<.005	Balance
3	6.0	2.0	4.0	1.9	.064	.02	.010	.06	.106		<.005	Balance
4	6.0	2.0	4.2	2.0	.070	.008	.009	.06	.10	.009	<.001	Balance
5	6.1	2.1	4.4	2.2	.080	.008	.004	.06	.10	.007	<.001	Balance

[a]Vendor-supplied information.

Table IV. Forming Parameters for Superplastic Straining Ti-6Al-2Sn-4Zr-2Mo Panels and Simulation Specimens

Panel	Specimen code	Strain rate, sec^{-1}	Forming time at 1650°F, hr
1	3F(100)-N	2×10^{-4}	$1\frac{1}{2}$
2	5F(400)-N	2×10^{-4}	$2\frac{3}{4}$
3	3F(100)-D	2×10^{-4}	$1\frac{1}{2}$
4	2F(125)-N	2×10^{-4}	$1\frac{1}{2}$
5	3F(200)-N	2×10^{-4}	$1\frac{3}{4}$
6	4F(200)-N	2×10^{-4}	2
7	5F(300)-D	1×10^{-4}	$4\frac{1}{4}$
8	5F(700)-D	1×10^{-4}	6
	3S(100)-N		$1\frac{1}{2}$
	3S(100)-D		$1\frac{1}{2}$
	5S(100)-N		$1\frac{1}{2}$
	5S(100)-D		$1\frac{1}{2}$
	5S(700)-D		6

Table V. Room-Temperature Tensile Properties of Ti-6Al-2Sn-4Zr-2Mo Sheet Material

Specimen code	Yield strength, ksi	Tensile strength, ksi	Young's modulus, ksi	Elongation in 2 inches, percent
As received				
2M(0)-N1	138.2	154.4	16.2×10^6	11.5
2M(0)-N2	141.7	156.5	16.3	15.0
3M(0)-N1	153.8	157.3	17.4	11.5
3M(0)-N2	154.7	157.2	17.4	12.0
3M(0)-N3	154.4	158.2	17.7	11.0
[a]3M(0)-N4	151.9	156.2	17.7	9.0
[a]3M(0)-N5	153.1	157.2	17.7	11.0
[a]3M(0)-N6	153.4	156.8	18.0	11.0
4D(0)-N1	135.6	147.5	16.2	12.5
4D(0)-N2	137.1	151.1	16.7	12.5
5D(0)-N1	134.0	143.9	16.3	11.0
5D(0)-N2	132.9	146.3	16.2	11.0
Duplex anneal[b]				
1M(0)-D1	145.2	150.9	17.1×10^6	14.0
1M(0)-D2	145.6	151.9	17.3	14.0
3M(0)-D1	148.1	152.5	17.7	12.5
3M(0)-D2	148.1	152.5	17.5	12.0
[a]3M(0)-D3	141.5	148.4	17.4	12.0
[a]3M(0)-D4	141.5	148.1	18.1	12.0
5D(0)-D1	136.7	150.1	17.5	12.5
5D(0)-D2	136.0	149.1	17.6	13.0
Superplastically formed				
3F(100)-N1	134.4	141.3	17.3×10^6	16.0
3F(100)-N2	131.6	141.6	17.5	12.5
3F(100)-N3	134.7	140.4	17.5	17.0
[a]3F(100)-N4	130.2	141.7	17.2	[c]12.5
[a]3F(100)-N5	131.3	140.6	16.6	15.0
[a]3F(100)-N6	133.6	141.5	16.7	[c]12.0
2F(125)-N1	130.0	141.3	16.3	15.5
2F(125)-N2	130.4	142.7	16.5	12.0
3F(200)-N1	136.3	147.7	18.5	[c]10.5
3F(200)-N2	134.1	144.0	18.0	[c]11.5
4F(200)-N1	131.4	143.2	16.2	10.0
4F(200)-N2	133.9	143.3	17.0	(c)
5F(400)-N1	130.9	140.6	17.0	(c)
5F(400)-N2	125.2	136.6	16.7	7.5
Superplastically formed + duplex anneal[b]				
3F(100)-D1	129.0	140.8	17.0×10^6	[c]9.0
3F(100)-D2	130.5	140.0	16.8	[c]9.5
[a]3F(100)-D3	134.4	144.0	17.1	[c]14.0
[a]3F(100)-D4	134.4	145.0	15.9	12.5
5F(300)-D1	128.2	137.7	17.8	[c]11.5
5F(700)-D1	121.4	131.2	16.7	[c]7.0
Simulation[d]				
5S(100)-N1	133.5	146.0	16.8×10^6	13.5
5S(100)-N2	133.2	145.7	16.6	13.5
5S(700)-N1	124.1	145.2	15.7	13.5
5S(700)-N2	123.8	145.3	15.9	13.0
Simulation[d] + duplex anneal[b]				
5S(100)-D1	135.1	146.7	16.7×10^6	12.0
5S(100)-D2	133.3	144.7	16.5	12.5

[a]Transverse test direction.
[b]1650°F, 1/4 hour; gas cool + 1450°F, 1/4 hour; gas cool.
[c]Specimen failed near shoulder.
[d]Forming temperature cycle without applied load.

Table VI. 600°F Tensile Properties Of Ti-6Al-2Sn-4Zr-2Mo Sheet Material

Specimen code	Yield strength, ksi	Tensile strength, ksi	Young's modulus, ksi	Elongation in 2 inches, percent
As received				
2M(0)-N1	96.5	121.1	15.1×10^6	[a]12.5
2M(0)-N2	95.7	119.6	15.2	13.0
3M(0)-N1	103.8	116.4	16.3	[a]11.5
3M(0)-N2	108.5	119.5	16.4	11.0
3M(0)-N3	106.3	119.1	16.4	11.5
[b]3M(0)-N4	102.5	115.1	16.1	10.0
[b]3M(0)-N5	103.5	112.6	16.0	10.0
[b]3M(0)-N6	101.9	113.2	16.3	10.0
5D(0)-N1	89.9	111.8	15.1	11.5
[c]5D(0)-N2		113.5		12.5
Duplex anneal[d]				
1M(0)-D1	94.9	108.9	17.2×10^6	13.0
1M(0)-D2	92.4	106.3	15.9	13.5
3M(0)-D1	102.0	116.8	17.1	12.0
3M(0)-D2	99.5	115.4	17.2	12.0
[b]3M(0)-D3	93.0	112.3	17.5	12.0
[b]3M(0)-D4	94.3	114.4	18.0	13.5
5D(0)-D1	92.2	115.6	17.5	12.0
5D(0)-D2	92.4	115.5	17.1	12.0
Superplastically formed				
[c]3F(100)-N1	89.6	107.5	16.5×10^6	[a]10.0
3F(100)-N2	89.8	109.1	16.5	[a]11.5
3F(100)-N3	82.7	110.6	16.7	12.0
[b]3F(100)-N4	87.9	111.8	15.9	
[b]3F(100)-N5	89.5	111.1	16.6	12.5
2F(125)-N1	84.7	106.8	15.0	13.0
3F(200)-N1	83.7	105.2	17.0	11.5
3F(200)-N2	86.8	108.1	16.9	12.0
4F(200)-N1	88.0	110.1	15.7	[a]8.5
4F(200)-N2	89.2	111.5	16.1	[a]11.0
5F(400)-N1	86.7	107.6	16.9	[a]9.0
5F(400)-N2	75.4	99.0	18.3	7.0
Superplastically formed + duplex anneal[d]				
3F(100)-D1	84.2	104.4	15.5×10^6	10.5
3F(100)-D2	84.8	104.3	15.4	12.5
[b]3F(100)-D3	86.8	108.4	15.4	12.0
[b]3F(100)-D4	88.5	108.9	15.3	12.5
5F(700)-D1	81.9	101.4	15.8	7.0
Simulation[e]				
3S(100)-N1	89.5	109.6	16.2×10^6	13.0
Simulation[e] + duplex anneal[d]				
3S(100)-D1	89.0	107.6	16.4×10^6	
3S(100)-D2	91.8	109.3	16.3	13.0

[a]Specimen failed near shoulder.
[b]Transverse test direction.
[c]Multiple heating and loading cycles.
[d]1650°F, 1/4 hour; gas cool + 1450°F, 1/4 hour; gas cool.
[e]Forming temperature cycle without applied load.

Table VII. 800°F Tensile Properties of Ti-6Al-2Sn-4Zr-2Mo Sheet Material

Specimen code	Yield strength, ksi	Tensile strength, ksi	Young's modulus, ksi	Elongation in 2 inches, percent
Duplex anneal[a]				
1M(0)-D1	86.5	102.9	12.8×10^6	16.5
Superplastically formed				
2F(125)-N1	79.6	98.5	12.1×10^6	18.5
3F(200)-N1	76.8	99.3	10.3	15.0

[a]1650°F, 1/4 hour; gas cool + 1450°F, 1/4 hour; gas cool.

Table VIII. 1000°F Tensile Properties of Ti-6Al-2Sn-4Zr-2Mo Sheet Material

Specimen code	Yield strength, ksi	Tensile strength, ksi	Young's modulus, ksi	Elongation in 2 inches, percent
Duplex anneal[a]				
[b]1M(0)-D1	75.7	94.5	10.5×10^6	21.5
Superplastically formed				
2F(125)-N1	74.8	95.4	11.5×10^6	17.5
3F(200)-N1	73.1	93.6	13.1	15.0

[a]1650°F, 1/4 hour; gas cool + 1450°F, 1/4 hour; gas cool.
[b]Strain rate of 0.0007 sec^{-1} was used for this test.

Table IX. 800°F Creep Properties of Ti-6Al-2Sn-4Zr-2Mo Sheet Material

Specimen code	Stress, ksi	Time, hr or (min), to creep strain of —							
		0.05%	0.10%	0.2%	0.3%	0.4%	0.5%	0.8%	1.0%
As received									
1M(0)-N1	80	(17)	1.4	5.0	10.5	20			
3M(0)-N1	90	(6.4)	(23)	1.0	2.1	3.6	5.3	12.0	17.5
3M(0)-N2	40	6.6	29.1						
3M(0)-N3	60	2.4	5.7	29.8					
5D(0)-N1	90	(1.1)	(13)	1.0	2.0	3.1			
5D(0)-N2	60	2.0	9.3						
5D(0)-N3	40	24.5	146						
5D(0)-N4	75	1.3	4.9	24.9	69.6	167			
Duplex anneal[a]									
1M(0)-D1	80	(9.6)	1.0	6.4	18.4	38.2	67		
1M(0)-D2	60	1.4	9.6						
3M(0)-D1	90	(1.0)	(5.7)	(27)	(53)	1.3	1.8	3.7	5.4
3M(0)-D2	90	(1.4)	(5.5)	(20)	(36)	(53)	1.2	2.8	4.9
5D(0)-D1	75	(35)	2.8	14.0	56.5	146			
5D(0)-D2	90	(3.2)	(30)	1.5	2.7	4.4	6.9	24.3	52.5
Superplastically formed									
3F(100)-N1	90	(7.8)	1.7	4.9	9.1	16.5	28.2	122	
3F(100)-N2	80	(49)	5.5	24.2	74.2				
2F(125)-N1	75	(58)	5.6	32.5					
2F(125)-N2	90	(6.3)	1.7	5.4	10.1	18.6	33.0		
3F(200)-N1	75	(52)	4.2	24.9	98.2				
3F(200)-N2	90	(30)	1.7	4.2	7.2	12.6	22.6		
4F(200)-N1	90	(2.2)	(31)	2.6	5.3	9.7	18.0	105	
4F(200)-N2	75	1.2	10.3	56.8					
5F(400)-N1	75	1.7	5.6	20.6	75.5				
Superplastically formed + duplex anneal[a]									
3F(100)-D1	75	(8.8)	(43)	2.5	6.8	18.8	39.7		
3F(100)-D2	90	(2.6)	(17)	(59)	1.9	3.1	4.8	13.6	23.6
5F(700)-D1	75	(2.0)	(24)	1.7	3.4	6.2	11.4		
Superplastically formed + triplex anneal[b]									
3F(100)-T1	75	(23)	2.94	24.7	74.7				
3F(100)-T2	90	(34)	(49)	1.4	2.8	4.5	6.7	15.6	26.1
Simulation[c]									
3S(100)-N1	90	(26)	1.1	2.0	3.0	4.5	6.6	25.4	81.9
Simulation[c] + duplex anneal[a]									
3S(100)-D1	75	(44)	2.44	12.0	40.4				
3S(100)-D2	90	(1.6)	(7.1)	(23)	(38)	(55)	1.3	3.3	6.3

[a]1650°F, 1/4 hour; gas cool + 1450°F, 1/4 hour; gas cool.
[b]1650°F, 1/4 hour; gas cool + 1450°F, 1/4 hour; gas cool + 1100°F, 2 hours; gas cool.
[c]Forming temperature cycle without applied load.

Table X. 1000°F Creep Properties of Ti-6Al-2Sn-4Zr-2Mo Sheet Material

Specimen code	Stress, ksi	Time, hr or (min), to creep strain of —							
		0.05%	0.10%	0.2%	0.3%	0.4%	0.5%	0.8%	1.0%
As received									
1M(0)-N1	40	(18)	1.0	4.2	10.6	20	31.5	61.2	76.4
2M(0)-N1	20	1.6	19.0	144					
2M(0)-N3	40	(53)	2.3	15.2	37.4	55.6	68.9	96.5	112
3M(0)-N1	20	(13)	(50)	3.0	6.1		20.1	38.1	
3M(0)-N2	40	(2.0)	(7.0)	(29)	1.1	1.9	2.9	6.1	8.6
3M(0)-N3	10	2.0	8.4	29.9	57.6	88.6	125		
4D(0)-N1	40	(20)	1.0	4.6	14.6	27.6	43.4	78.0	96.8
4D(0)-N2	50	(3.9)	(15)	1.1	2.9	5.5	9.6		
5D(0)-N1	20	(13)	1.8	11.2	31.0	69.8	120		
5D(0)-N2	30	(8.6)	(30)	4.1	12.7	26.0	41.9	91.6	124
5D(0)-N3	40	(3.5)	(19)	1.5	4.2	9.6	15.1	35.7	50.7
Duplex anneal[a]									
1M(0)-D1	40	(10)	(35)	2.5	6.2	12.3	20.4	48.4	65.6
1M(0)-D2	30	(16)	1.2	7.8	21.2	38.7	58.5	119	
3M(0)-D1	40	(1.6)	(14)	1.2	3.0	5.8	9.2	23.5	32.8
3M(0)-D2	30	(12)	(41)	3.6	8.2	14.6	22.9	50.2	70.4
3M(0)-D3	20	(27)	2.2	11.0	25.3	44.0	64.0	122	
5D(0)-D1	20	1.2	6.9	30.1	72.5	135	210		
5D(0)-D2	40	(7.8)	(27)	1.7	4.6	9.9	17.6	44.3	63.4
5D(0)-D3	50	(3.6)	(15)	1.3	3.5	6.8	11.2	25.1	34.1
Superplastically formed									
3F(100)-N1	40	1.3	4.6	21.1	46.5	66.0	82.0		
3F(100)-N2	60	(1.2)	(24)	2.6	9.2	18.8	26.1	38.8	44.4
2F(125)-N1	60	(5.5)	(30)	2.9	7.9	14.9	22.0	37.6	45.3
2F(125)-N2	40	1.1	6.0	39.8					
2F(125)-N3	30	3.1	25.0	120	176	224			
3F(200)-N1	60	(.48)	(17)	2.6	9.6	19.2	29.0		
3F(200)-N2	40	1.2	8.3	53.6	90.6	115	139	188	
3F(200)-N3	50	(15)	1.5	8.5	29.3	46.9	60.1	87.0	101
4F(200)-N1	60	(8.2)	(34)	3.3	9.2	17.8	25.4	40.1	46.0
4F(200)-N2	40	1.8	11.3	54.5	86.5	108			
4F(200)-N3	50	(20)	1.9	16.6	36.8	50.3	60.6	82.0	93.1
5F(200)-N1	40	2.1	15.7	70.0	102	122	138		
5F(200)-N2	60	(4.5)	(20)	1.6	4.2	7.9	11.9	21.7	26.3
Superplastically formed + duplex anneal[a]									
3F(100)-D1	60	(.90)	(3.1)	(7.5)	(16)	(28)	(43)	1.8	2.9
3F(100)-D2	40	(5.5)	(23)	1.7	5.2	11.2	19.2	50.4	71.3
3F(100)-D3	30	(19)	1.4	10.0	27.7	51.9	75.7		
5F(300)-D1	60	(1.1)	(3.7)	(12)	(26)	(45)	1.1	2.6	3.9
5F(700)-D1	40	(2.4)	(9.3)	1.0	2.2	4.8	9.8	27.6	43.5
Superplastically formed + triplex anneal[b]									
3F(100)-T1	40	(6.9)	(38)	3.0	8.1	15.4	24.0	55.3	75.3
3F(100)-T2	40	(9.0)	(41)	3.5	8.4	16.3	25.6	53.4	
Simulation[c]									
5S(100)-N1	40	1.1	5.7	59.1					
5S(100)-N2	60	(19)	1.2	6.9	20.6	32.3	42.0	59.2	67.7
Simulation[c] + duplex anneal[a]									
5S(100)-D1	40	(1.6)	(12)	1.4	5.3	13.7	25.7	67.6	
5S(100)-D2	60	(2.8)	(9.9)	(36)	1.4	2.6	4.0	9.9	13.7

[a] 1650°F, 1/4 hour; gas cool + 1450°F, 1/4 hour; gas cool.
[b] 1650°F, 1/4 hour; gas cool + 1450°F, 1/4 hour; gas cool + 1100°F, 2 hours; gas cool.
[c] Forming temperature cycle without applied load.

Table XI. Quantitative Metallographic Findings of Ti-6Al-2Sn-4Zr-2Mo Sheet Material

Specimen code	Primary alpha, percent	Transformed beta,[a] percent	Grain size, μm
1M(0)-N	84	30–70	4.5
2M(0)-N	77	70	6.3
3M(0)-N	85	0	3.7
4D(0)-N	81	50	4.9
5D(0)-N	85	0	3.1
1M(0)-D	83	30	4.9
3M(0)-D	82	20	4.2
5D(0)-D	87	0	3.0
3F(100)-N	83	90	5.2
2F(125)-N	83	90	6.9
3F(200)-N	80	80	6.8
4F(200)-N	86	70	6.9
5F(400)-N	86	90	7.0
3F(100)-D	83	90	6.7
5F(300)-D	82	90	9.3
5F(700)-D	81	99	11.8
3S(100)-N	85	0	5.1
5S(100)-N	84	0	4.0
5S(700)-N	84	0	4.8
3S(100)-D	80	30	5.1
5S(100)-D	84	10	4.6

[a]Percent of beta phase region which has transformed to alpha plus beta.

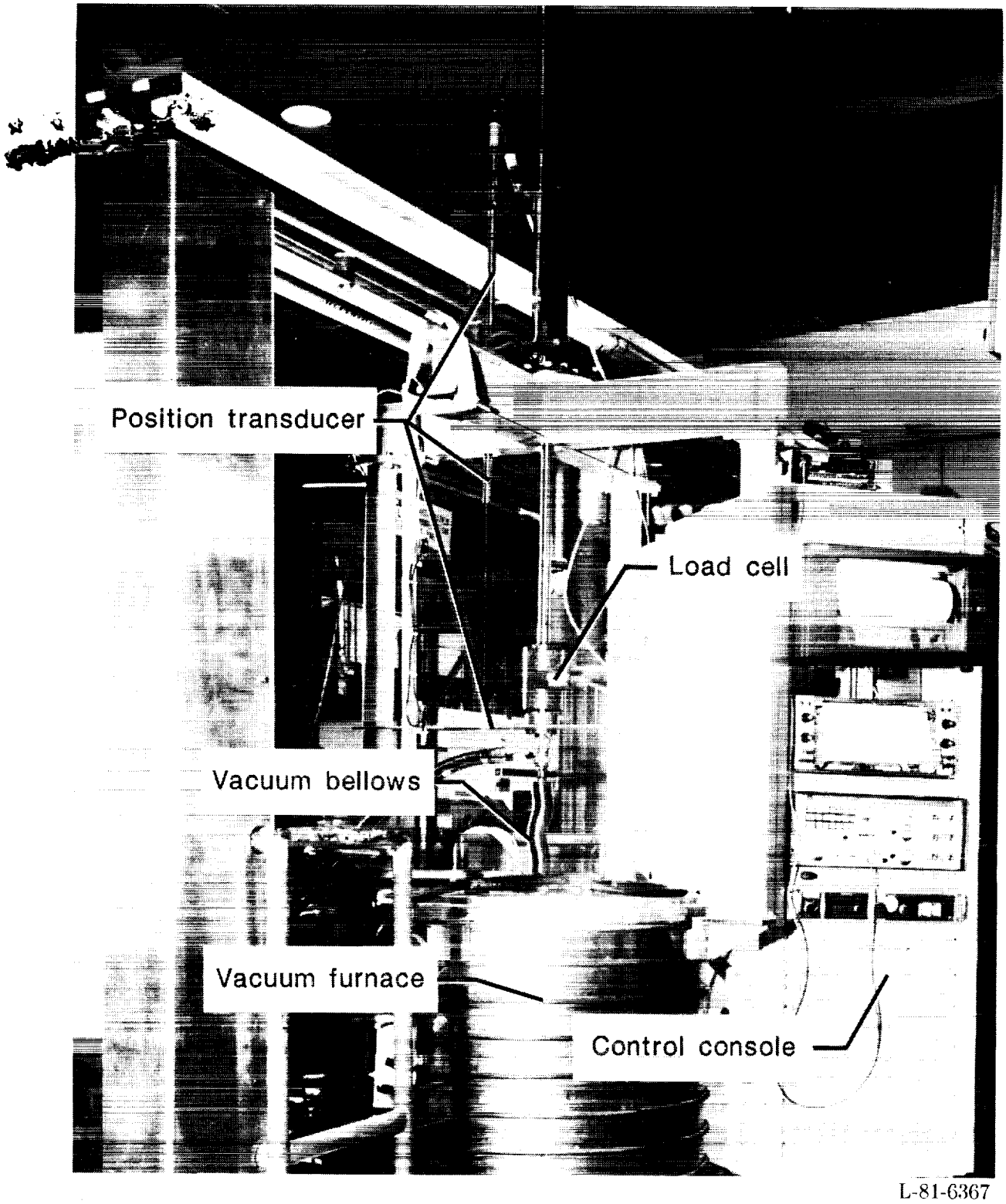

Figure 1. Axial superplastic forming apparatus.

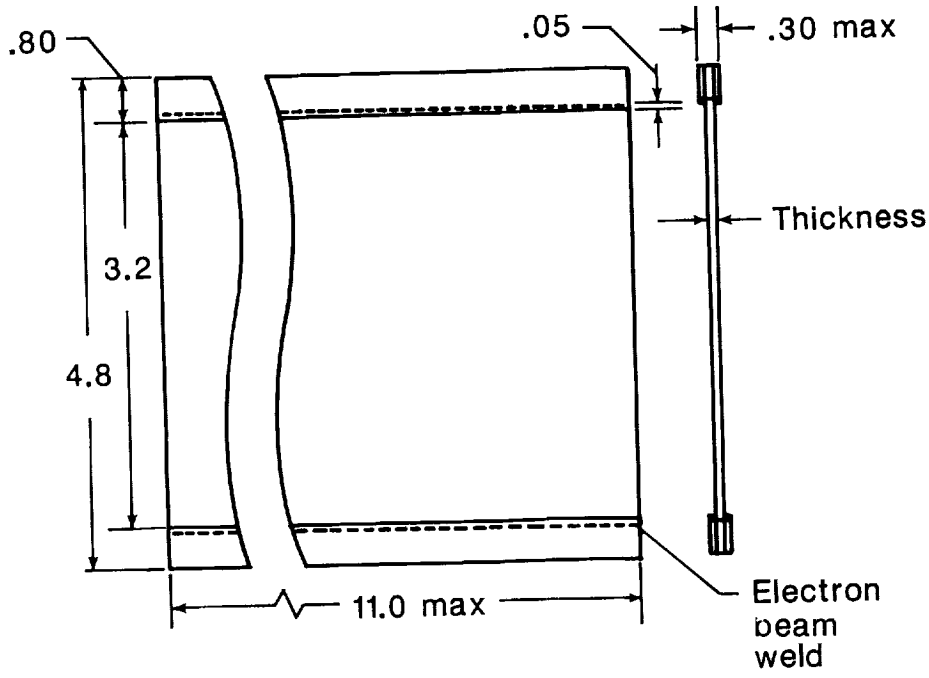

(a) Schematic drawing of panel. Dimensions are in inches.

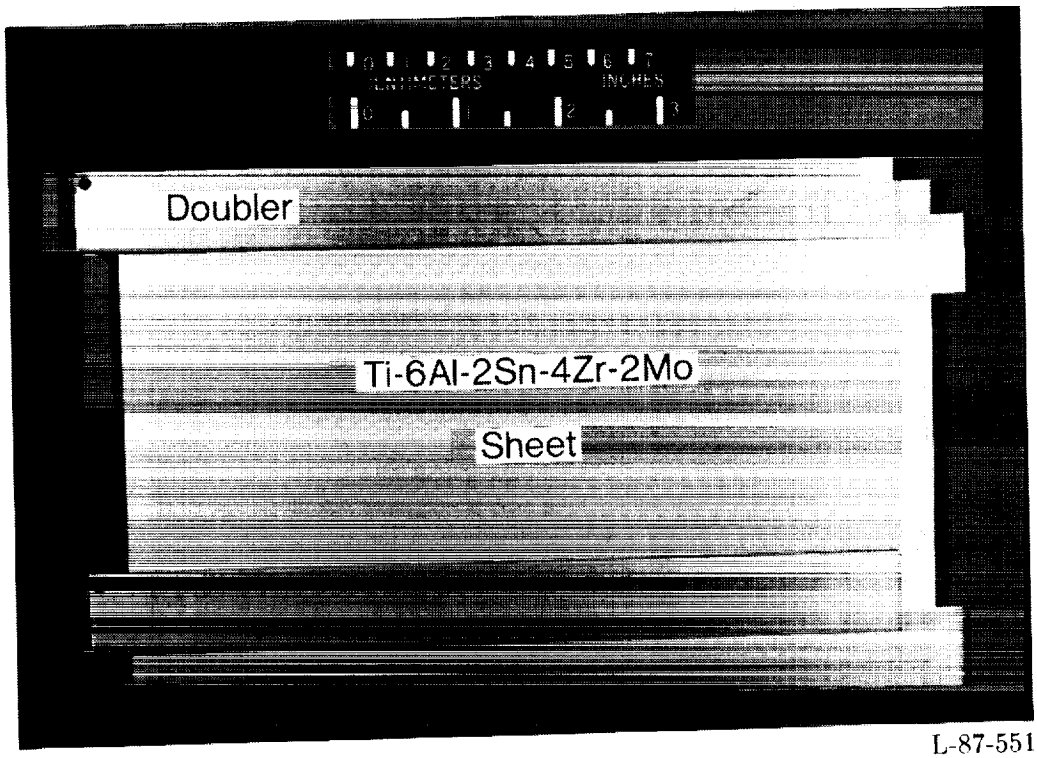

(b) Panel components.

Figure 2. Panel configuration for axial superplastic forming 400 percent.

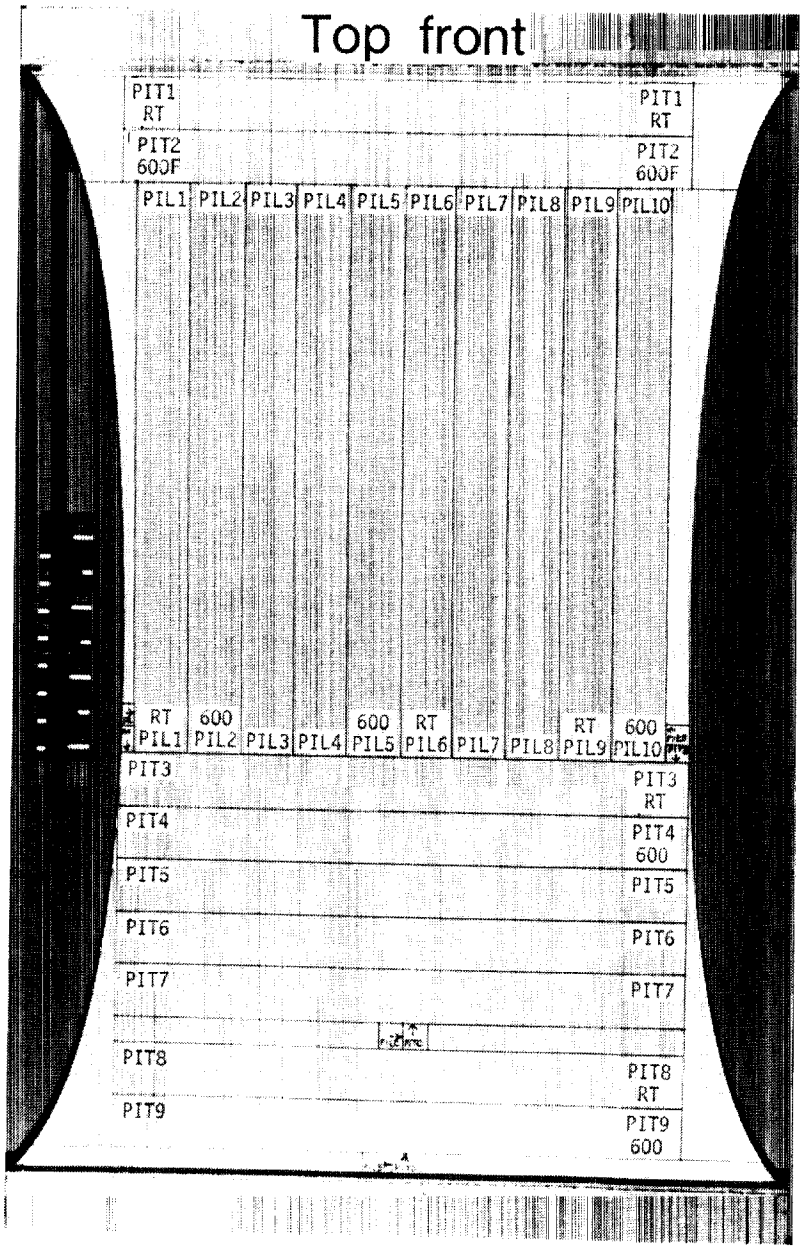

(a) Strained 100 percent. L-83-3575

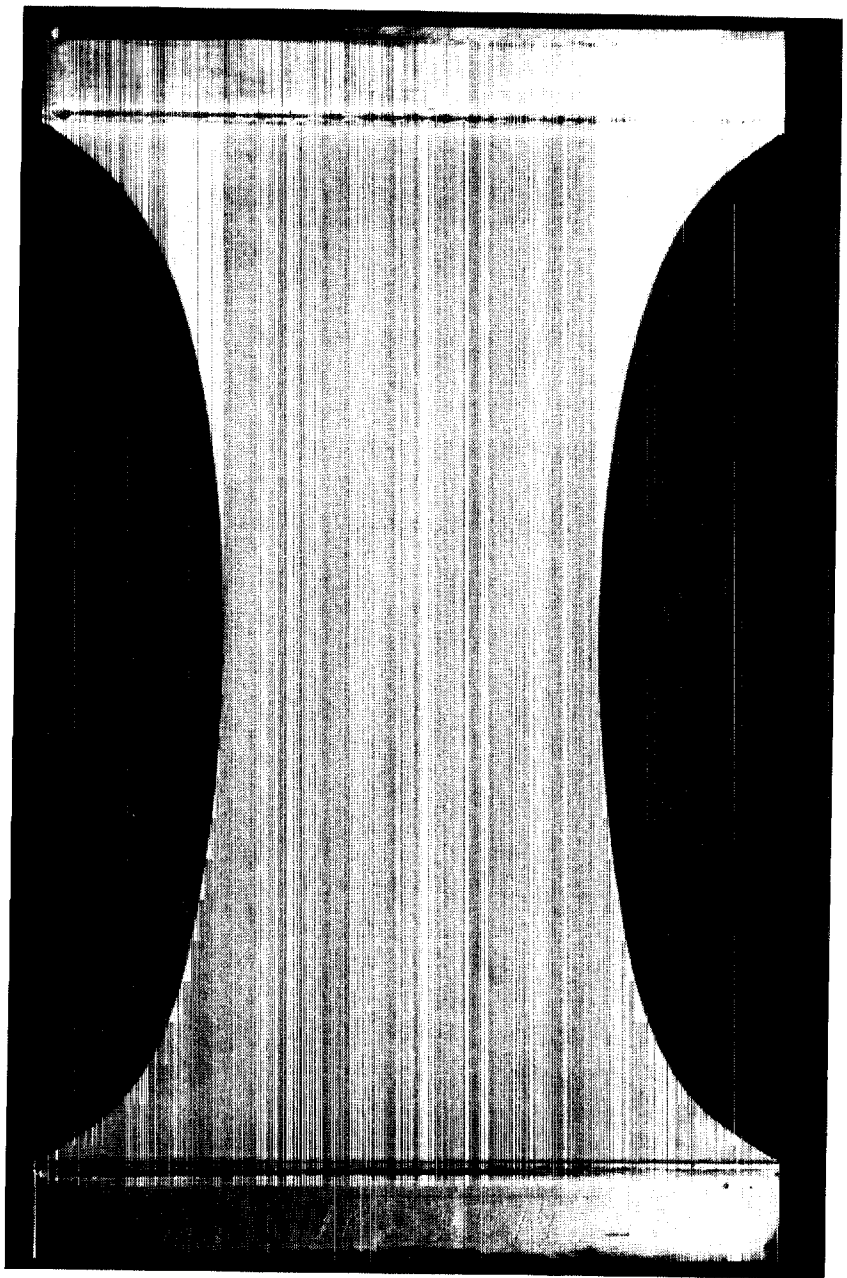

(b) Strained 700 percent. L-83-8723

Figure 3. Superplastically formed Ti-6Al-2Sn-4Zr-2Mo panels.

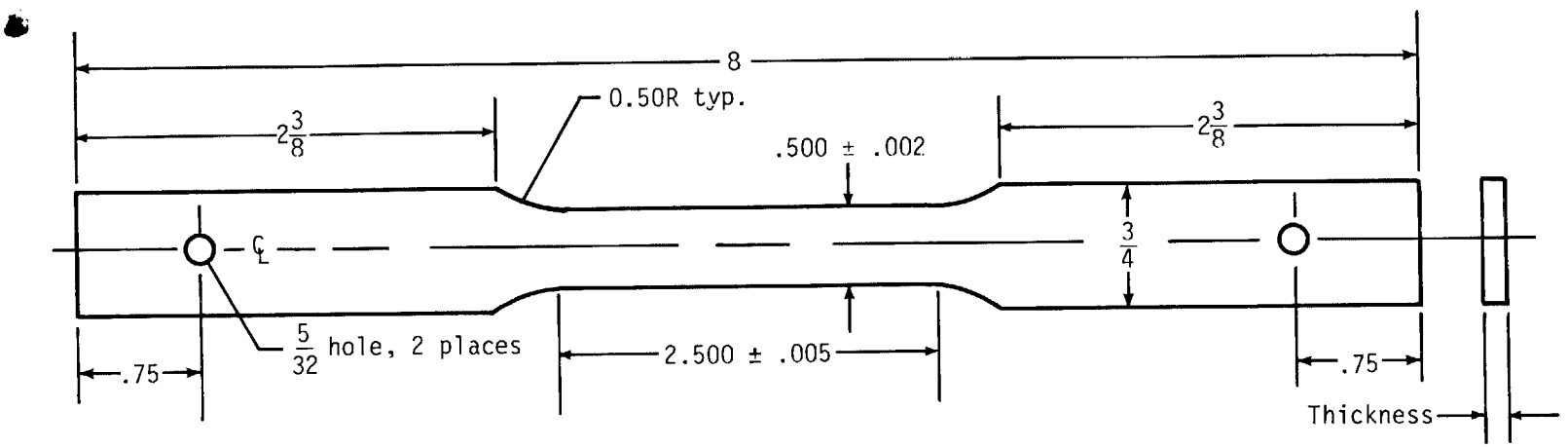

Figure 4. Specimen configuration for tensile and creep tests. Dimensions are in inches.

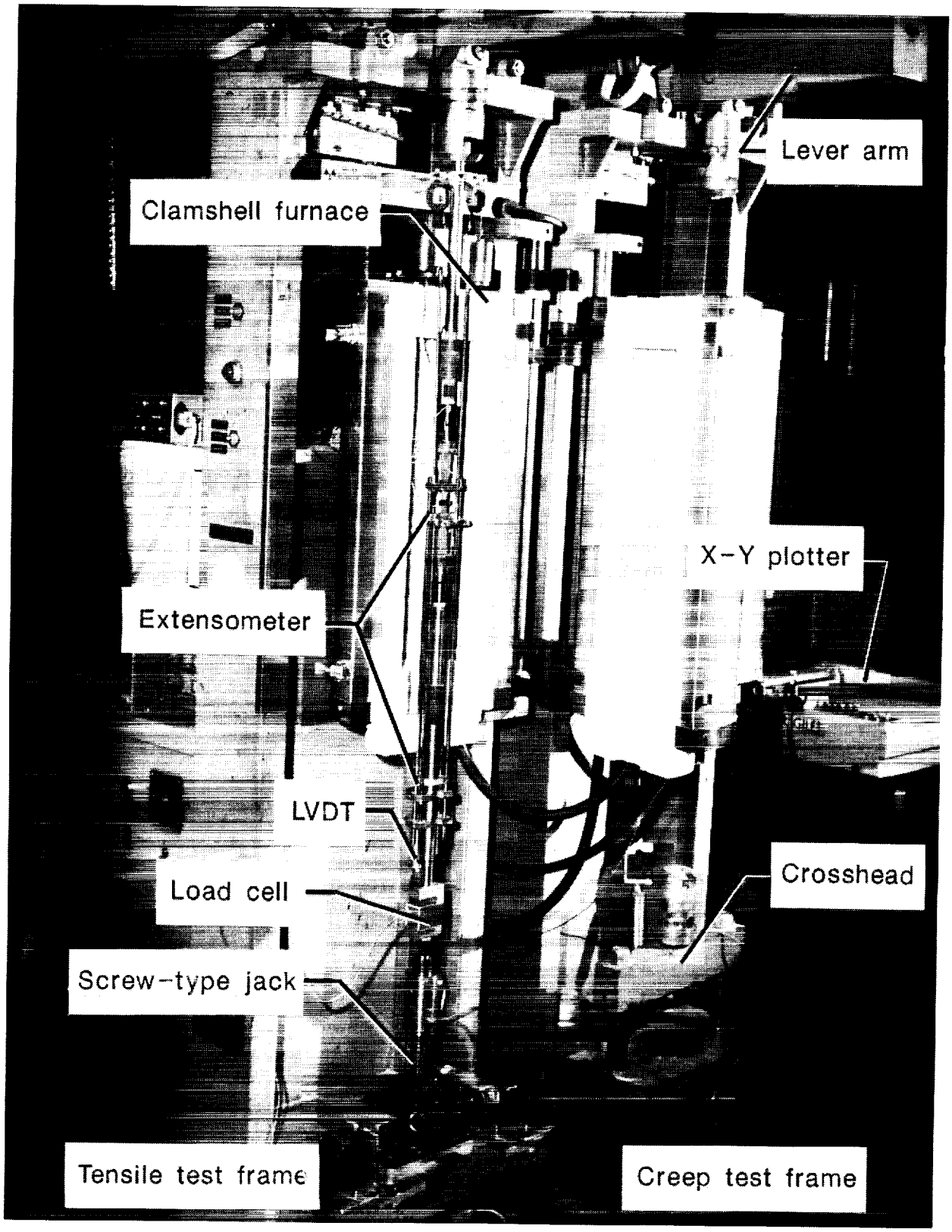

L-83-10,478

Figure 5. Elevated-temperature test equipment for Ti-6Al-2Sn-4Zr-2Mo tensile and creep tests.

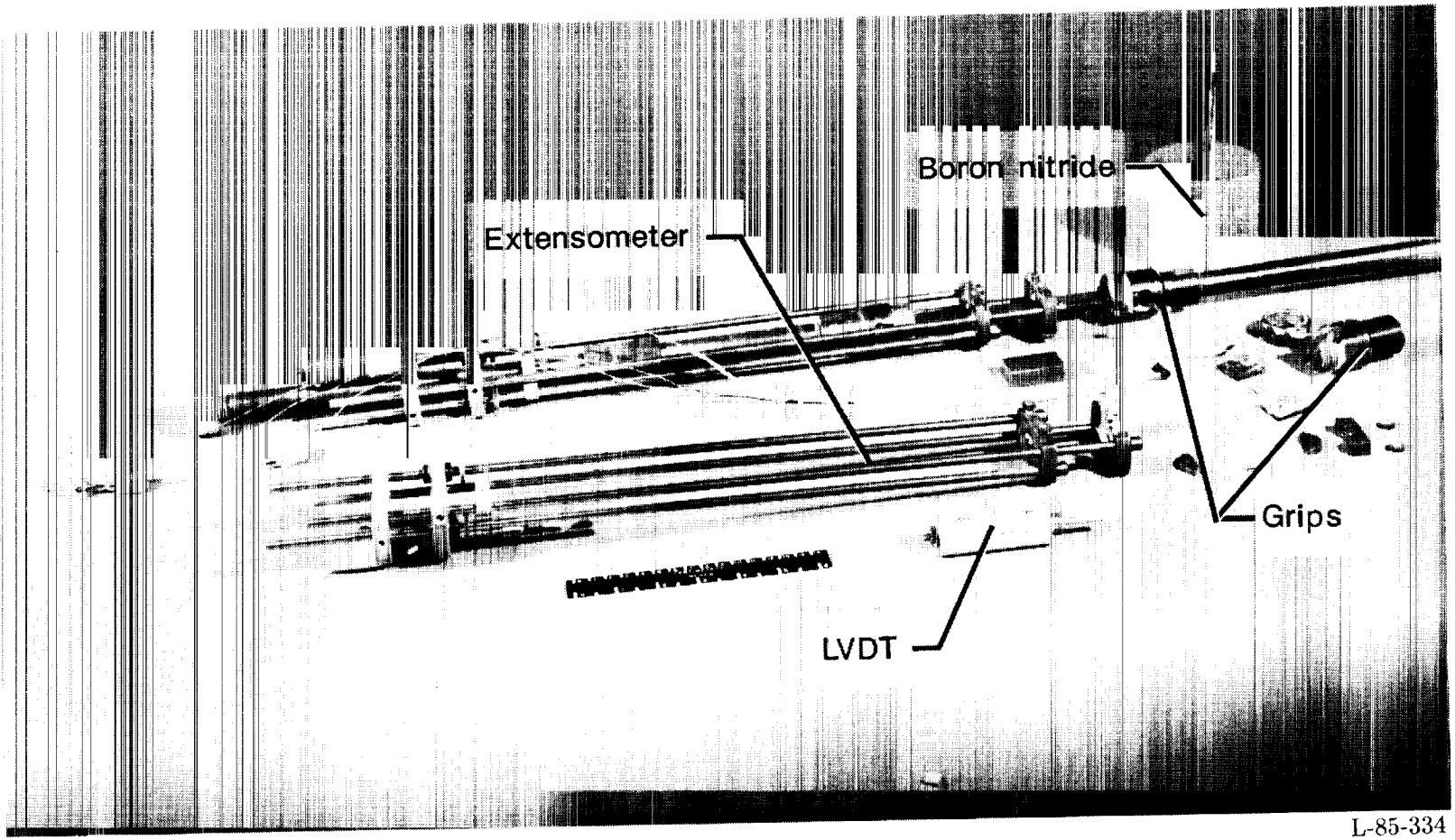

Figure 6. Extensometer, LVDT, and specimen grips used for elevated-temperature tensile and creep tests.

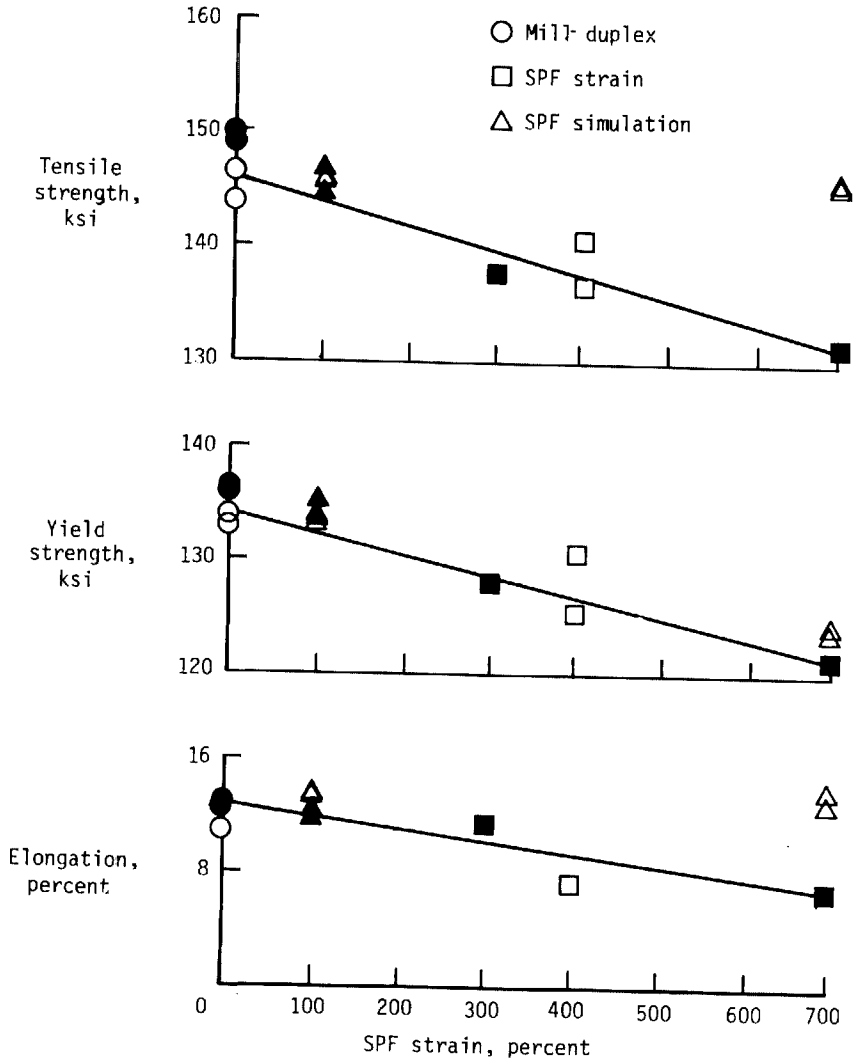

Figure 7. Effect of SPF strain on room-temperature properties of Ti-6242 sheet from heat 5. Solid symbols indicate duplex annealed after indicated treatment.

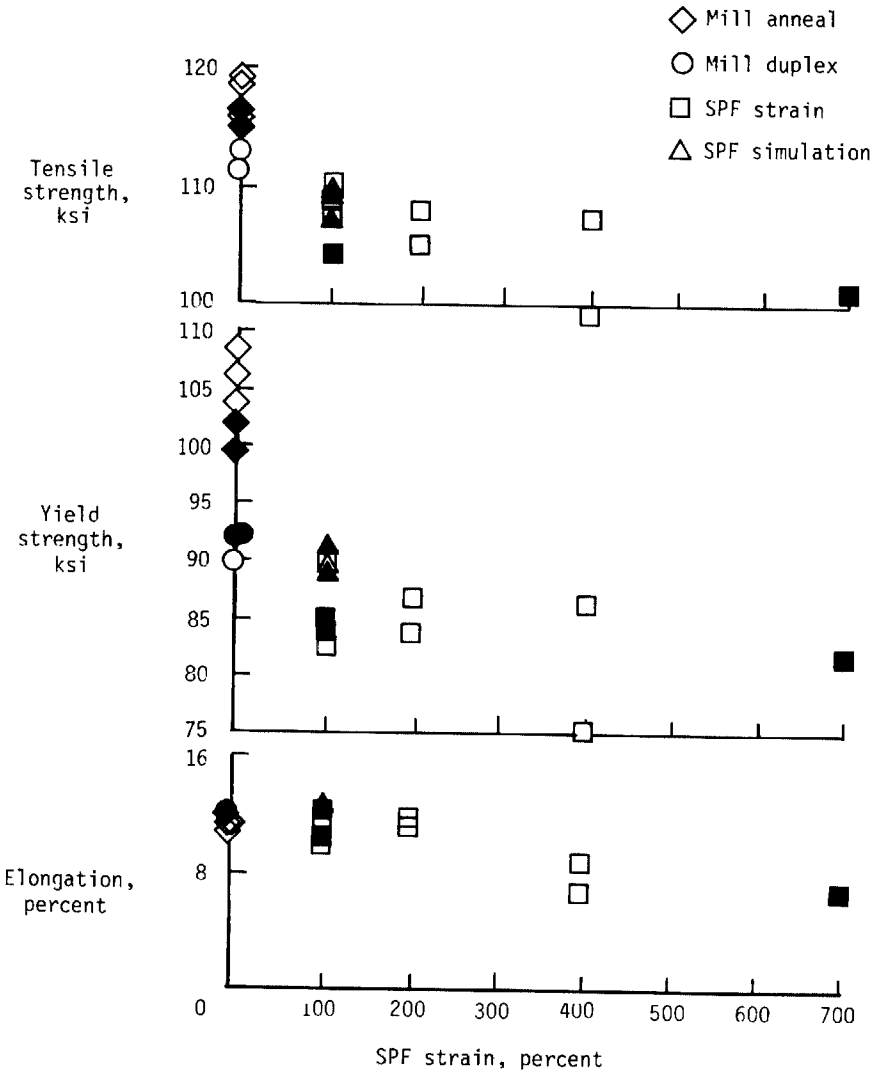

Figure 8. Effect of SPF strain on 600°F tensile properties of Ti-6242 sheet. Solid symbols indicate duplex annealed after indicated treatment.

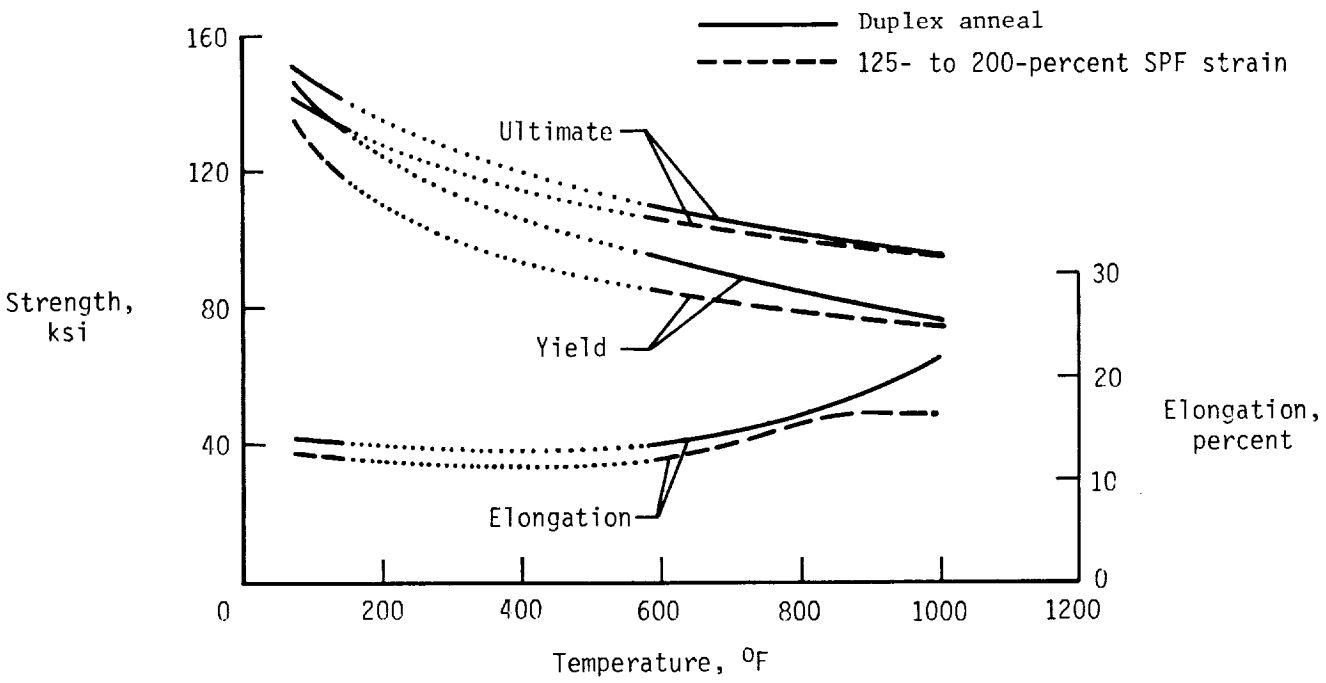

Figure 9. Elevated-temperature tensile properties of Ti-6242 sheet with and without SPF.

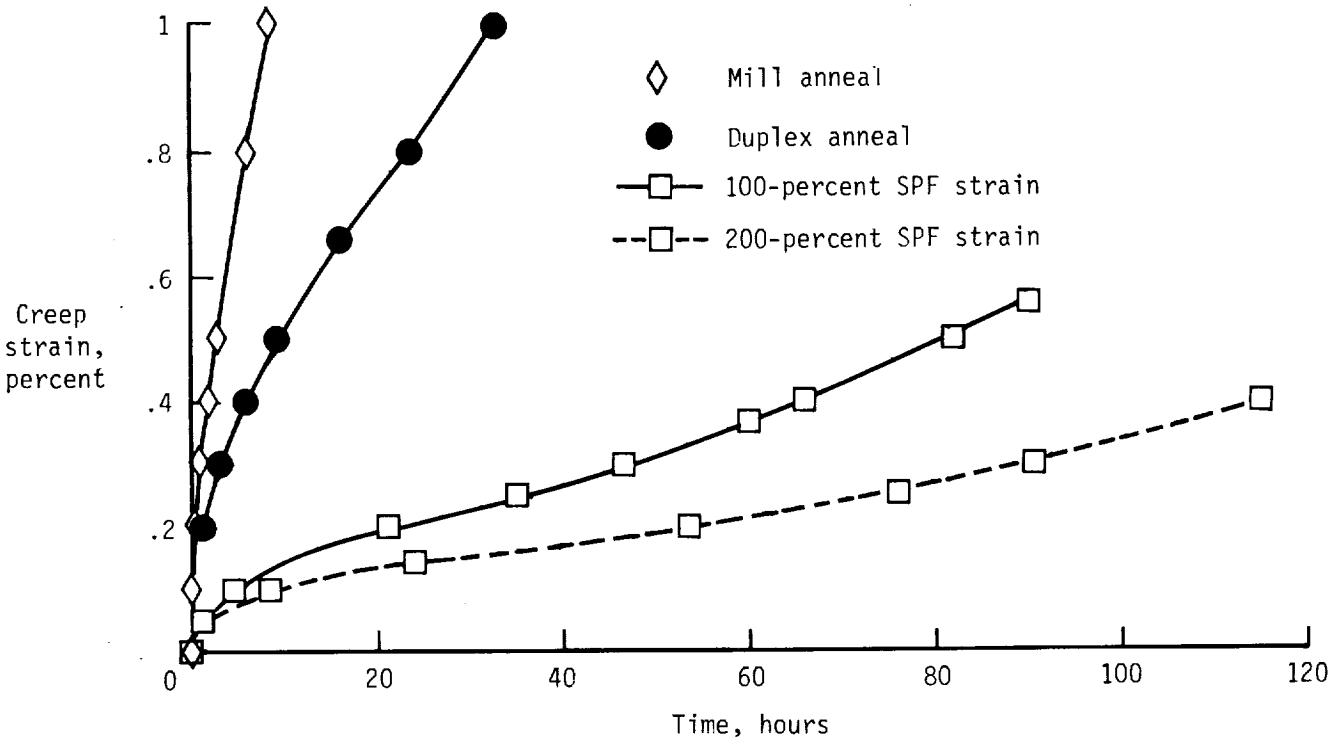

Figure 10. Effect of superplastic forming (SPF) on creep behavior of Ti-6242 at 1000°F and 40 ksi stress. Heat 3.

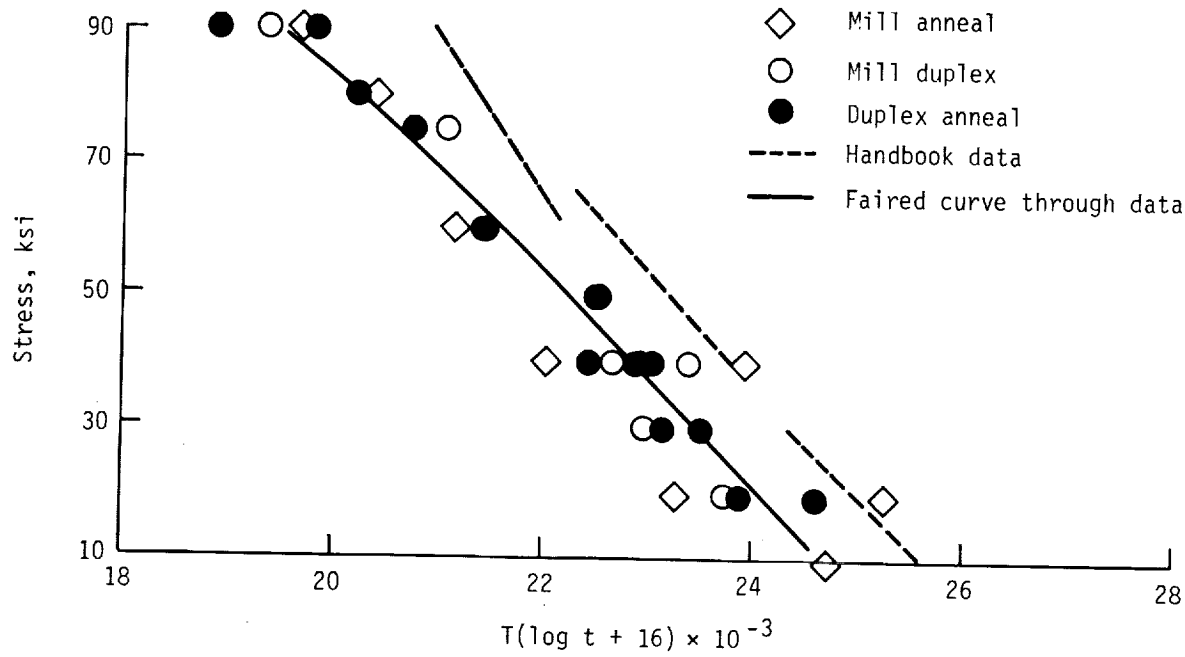

Figure 11. Larson-Miller plot of 0.1-percent creep data for Ti-6242 sheet.

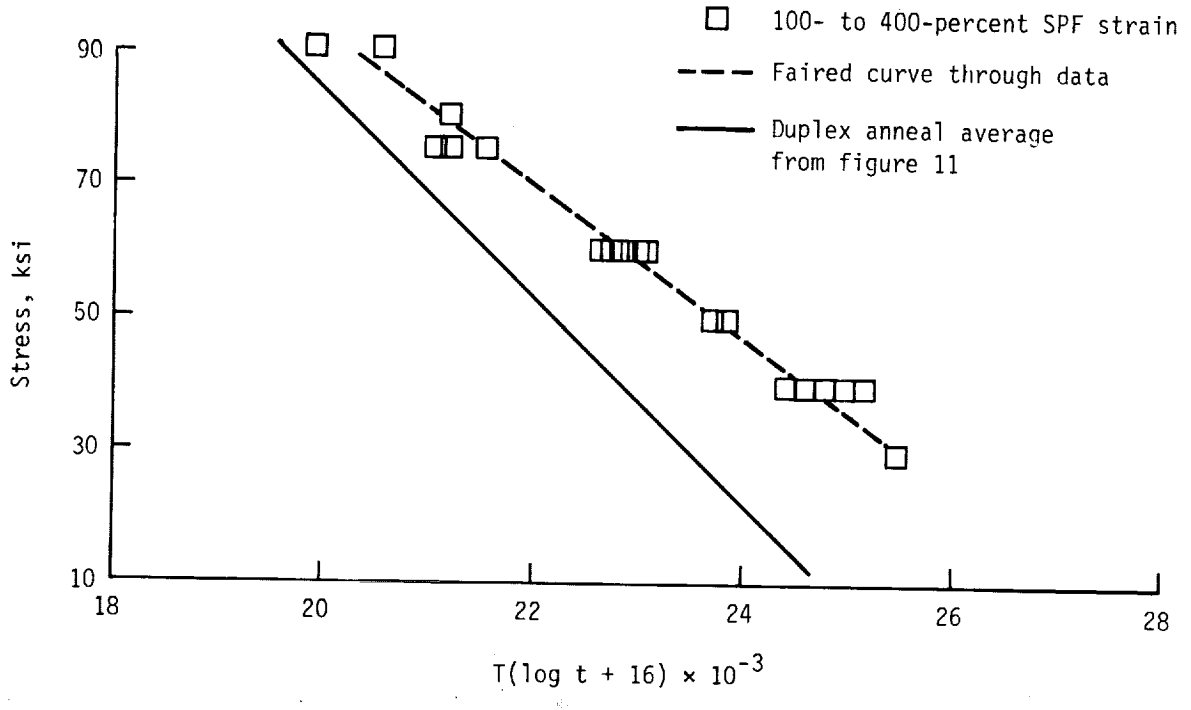

Figure 12. Larson-Miller plot of 0.1-percent creep data for Ti-6242 sheet after SPF processing.

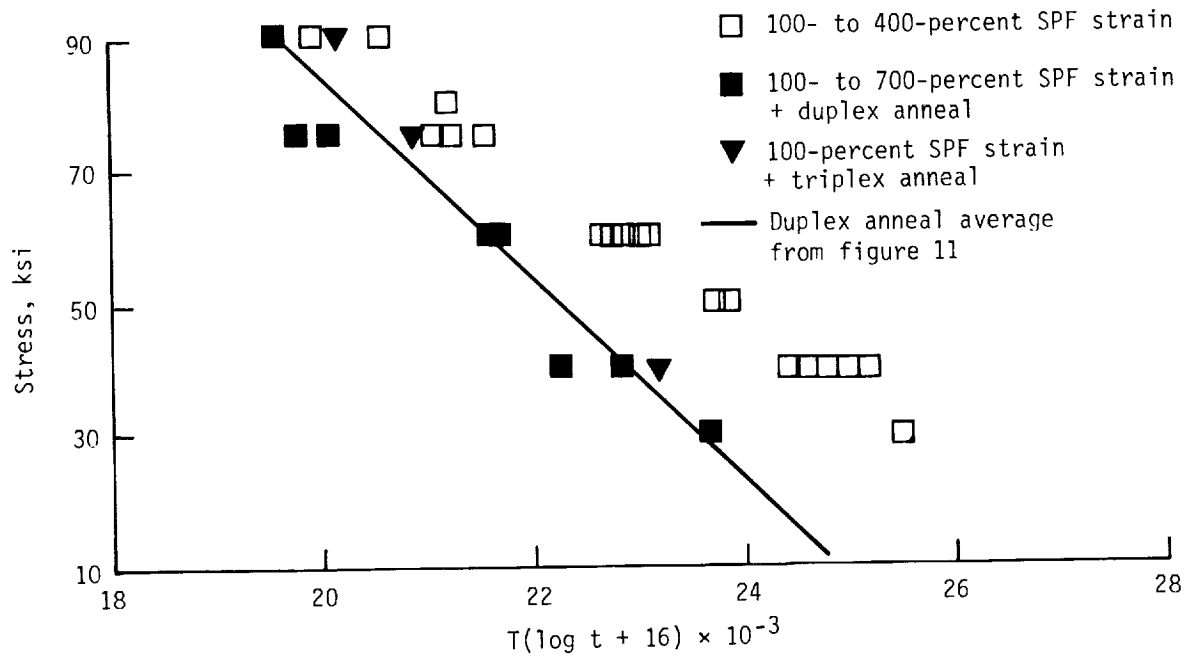

Figure 13. Larson-Miller plot of 0.1-percent creep data for Ti-6242 sheet after SPF processing, with and without heat treatment.

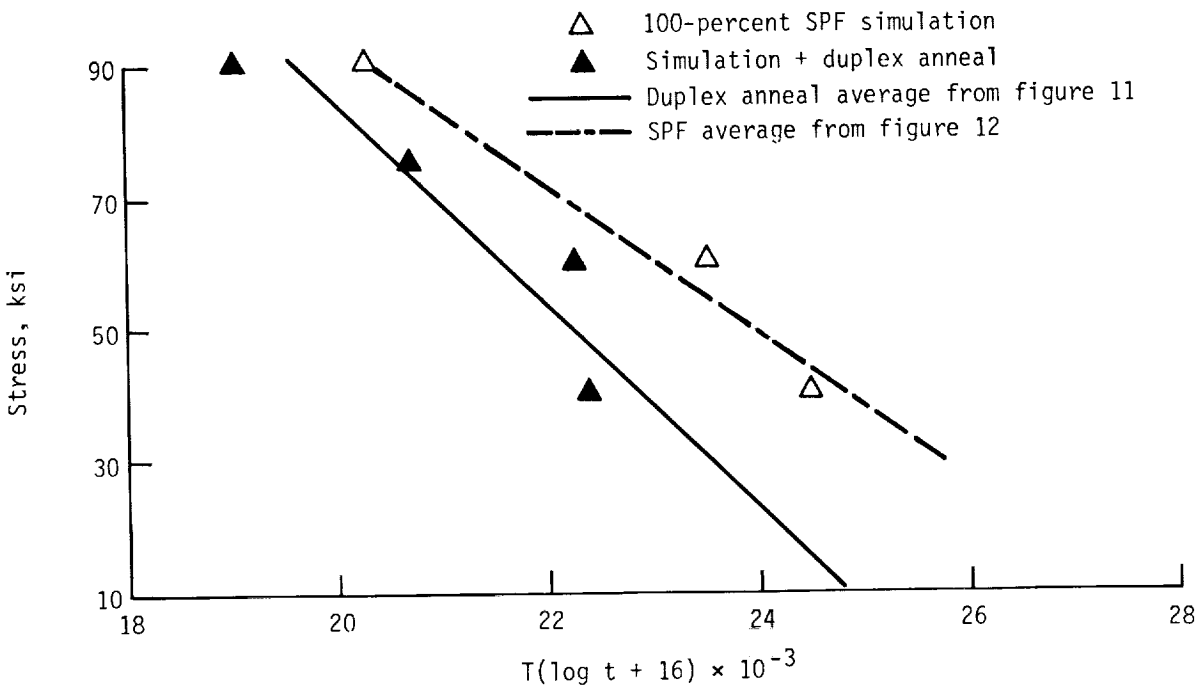

Figure 14. Larson-Miller plot of 0.1-percent creep data for Ti-6242 sheet after SPF simulation.

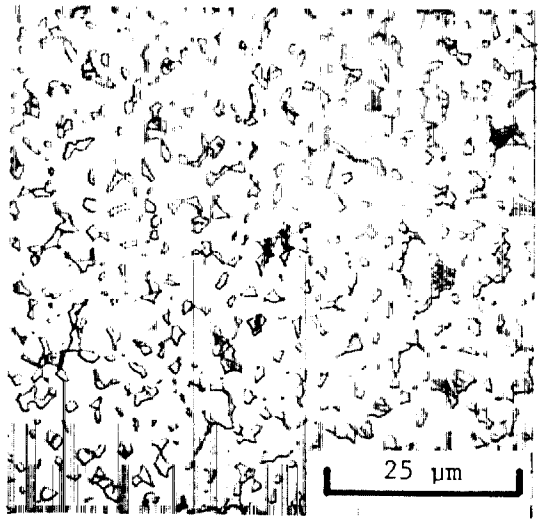

(a) Heat 1; mill anneal.

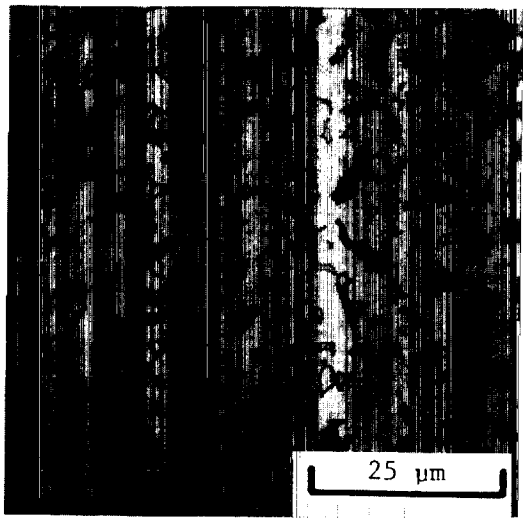

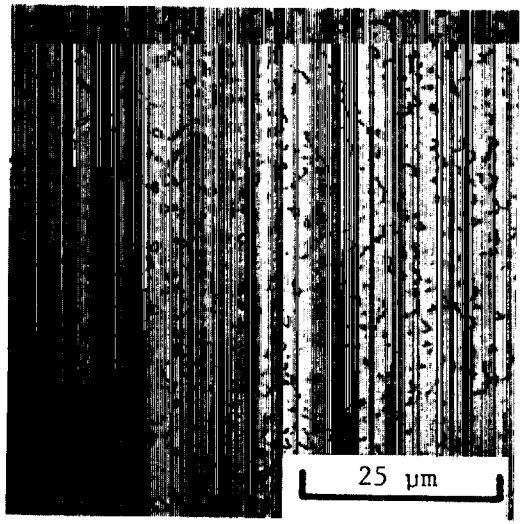

(b) Heat 2; mill anneal.

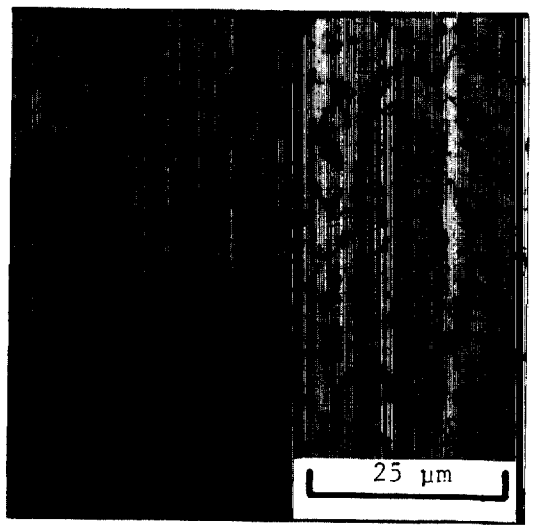

(d) Heat 4; mill duplex.

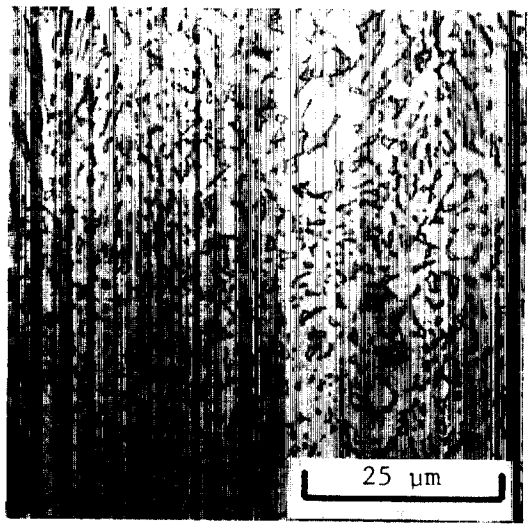

(e) Heat 5; mill duplex.

L-87-544

Figure 15. Photomicrographs of longitudinal sections of as-received Ti-6242 sheet. Kroll's reagent.

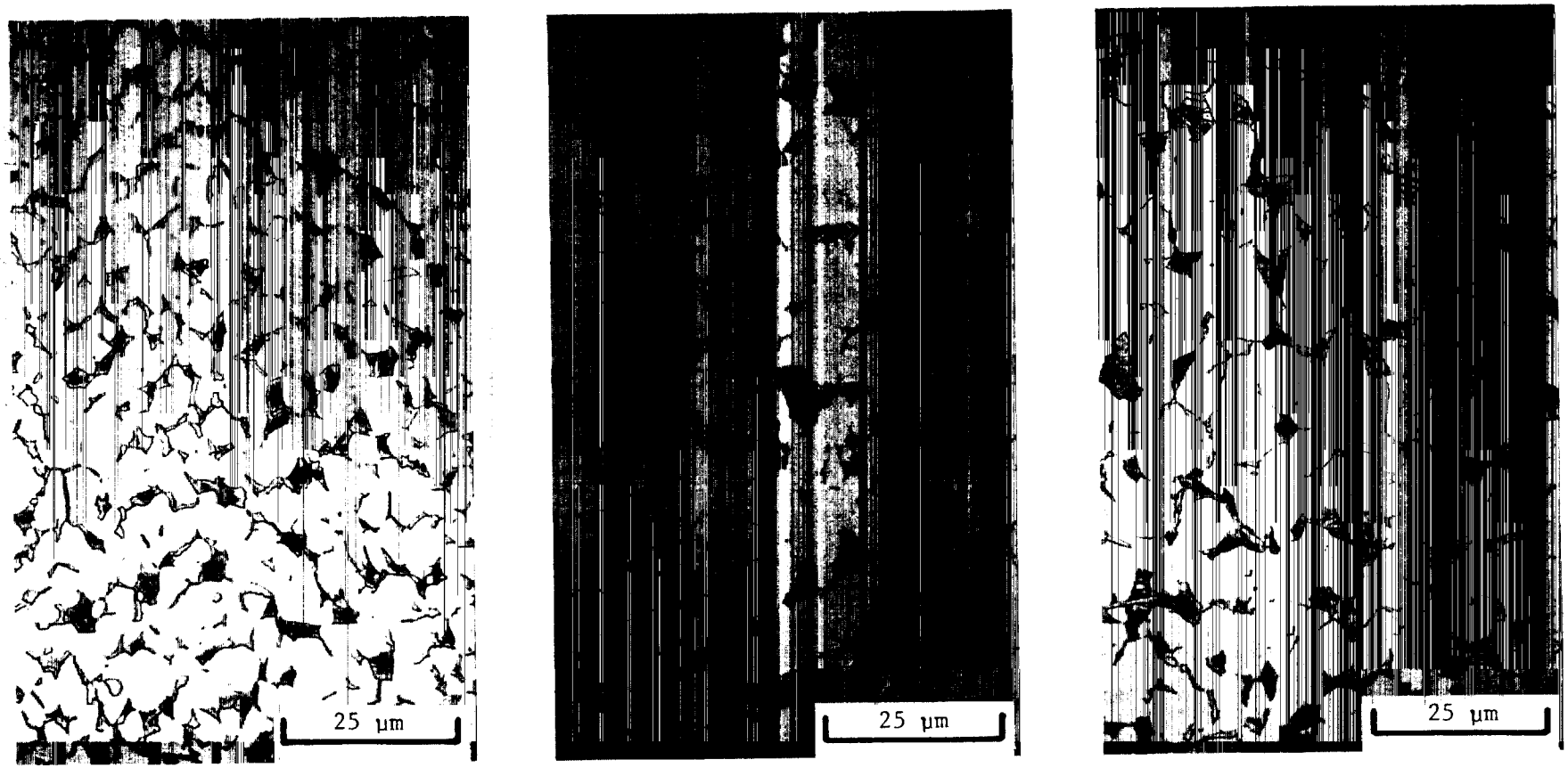

(a) 100-percent SPF strain.

(b) 200-percent SPF strain.

(c) 400-percent SPF strain.

L-87-545

Figure 16. Typical microstructure of longitudinal sections of SPF Ti-6242 sheet. Kroll's reagent.

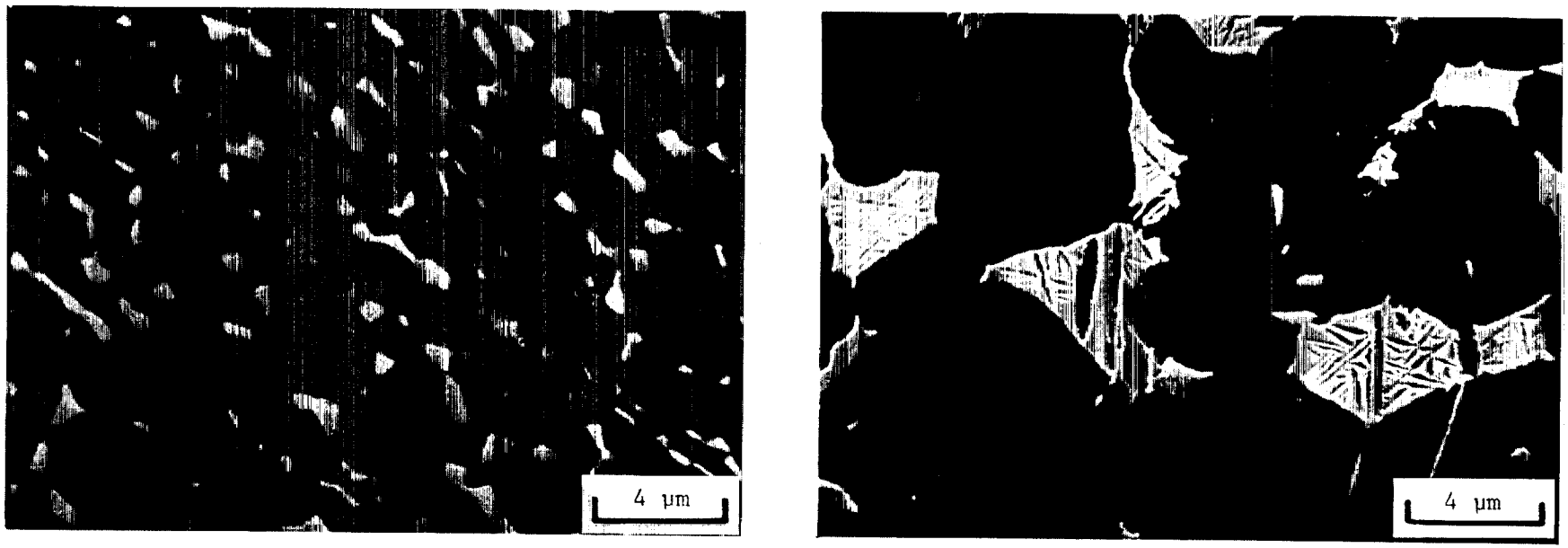

(a) Mill anneal.

(b) 100-percent SPF strain.

L-87-546

Figure 17. SEM micrographs comparing longitudinal sections of mill-anneal and SPF Ti-6242 sheet. Kroll's reagent.

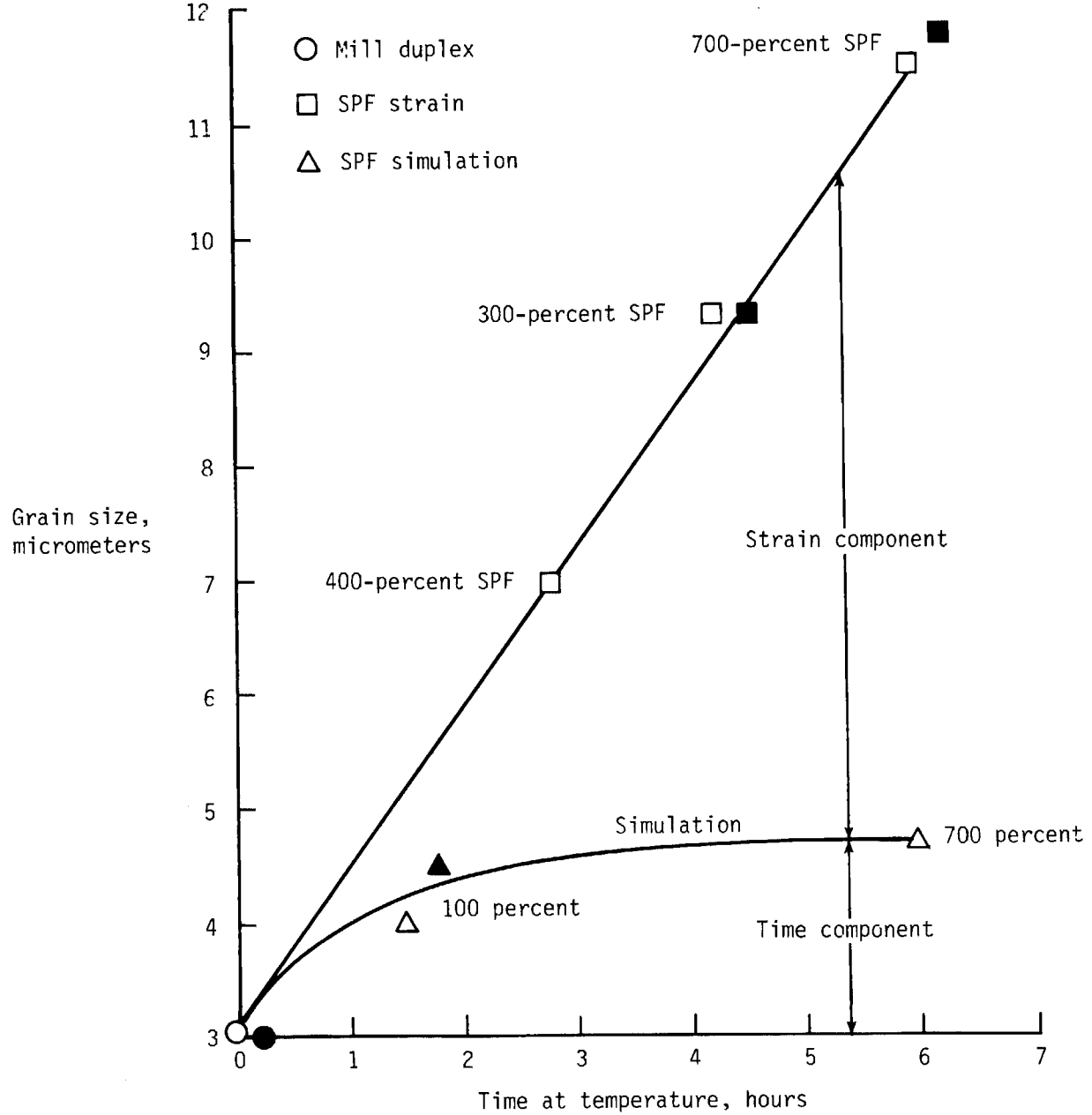

Figure 18. Effect of 1650°F exposure on grain size of Ti-6242 sheet with and without superplastic forming. Heat 5.

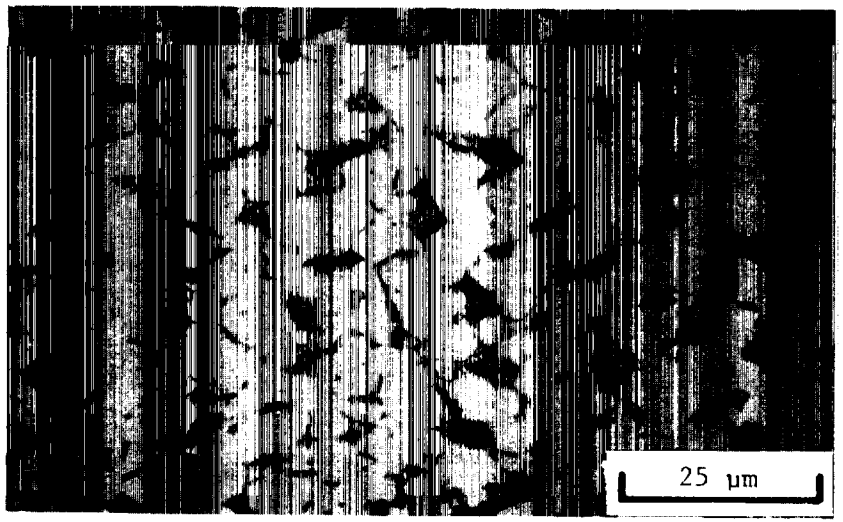

(a) 200-percent SPF strain.

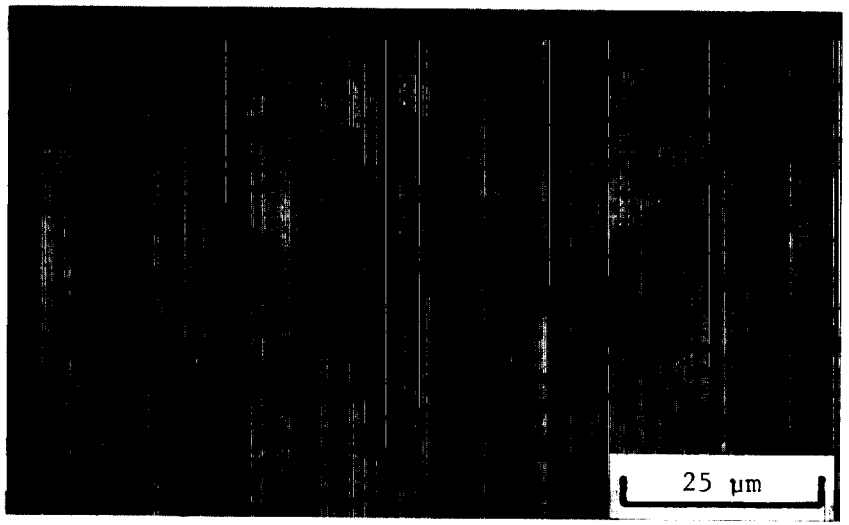

(b) 800°F tensile.

(c) 1000°F creep.

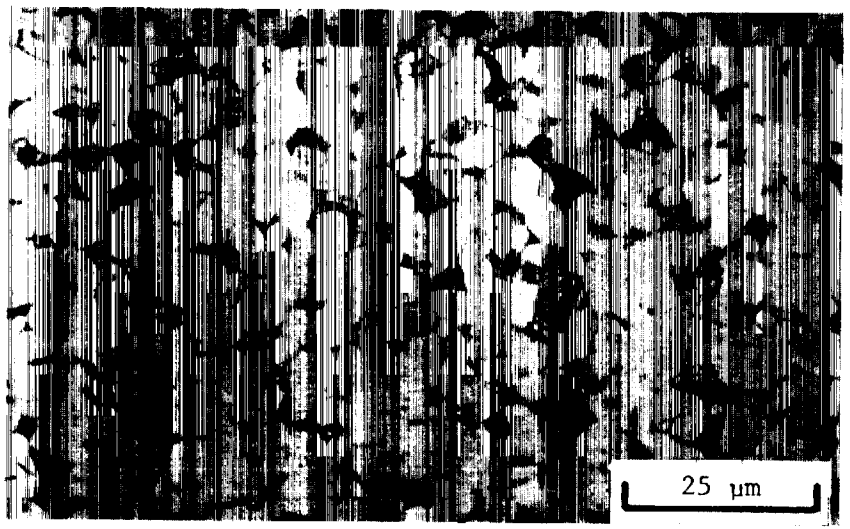

(d) 800°F creep.

L-87-547

Figure 19. Effect of test condition on microstructure of longitudinal sections of SPF Ti-6242 sheet. Kroll's reagent.

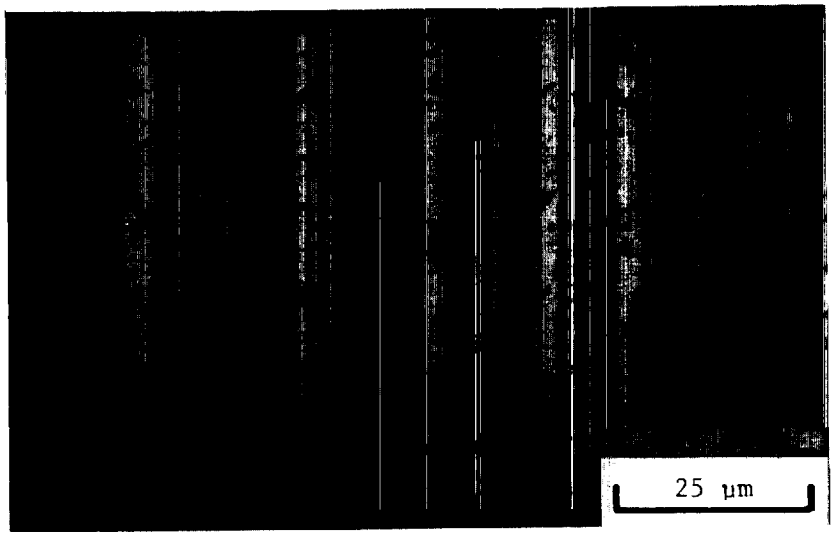

(a) 100-percent SPF strain.

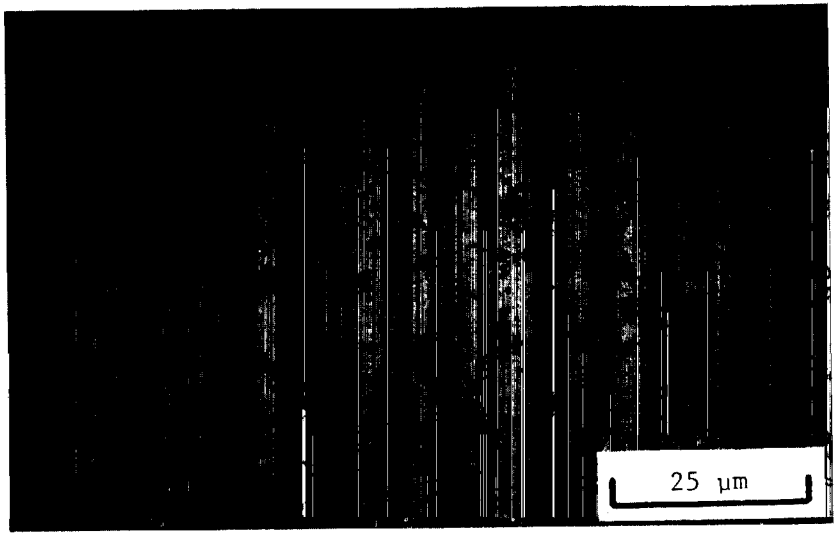

(b) 100-percent SPF strain + duplex anneal.

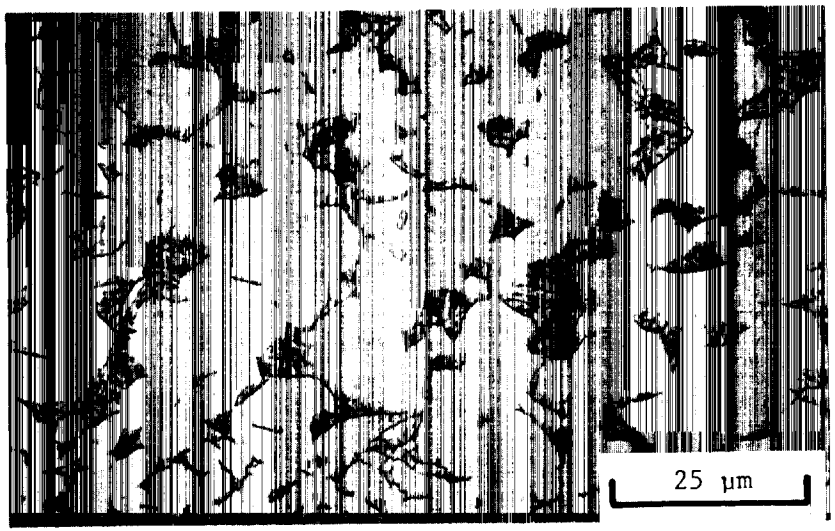

(c) 700-percent SPF strain.

(d) 700-percent SPF strain + duplex anneal.

L-87-548

Figure 20. Photomicrographs of longitudinal sections of SPF Ti-6242 with and without duplex anneal. Kroll's reagent.

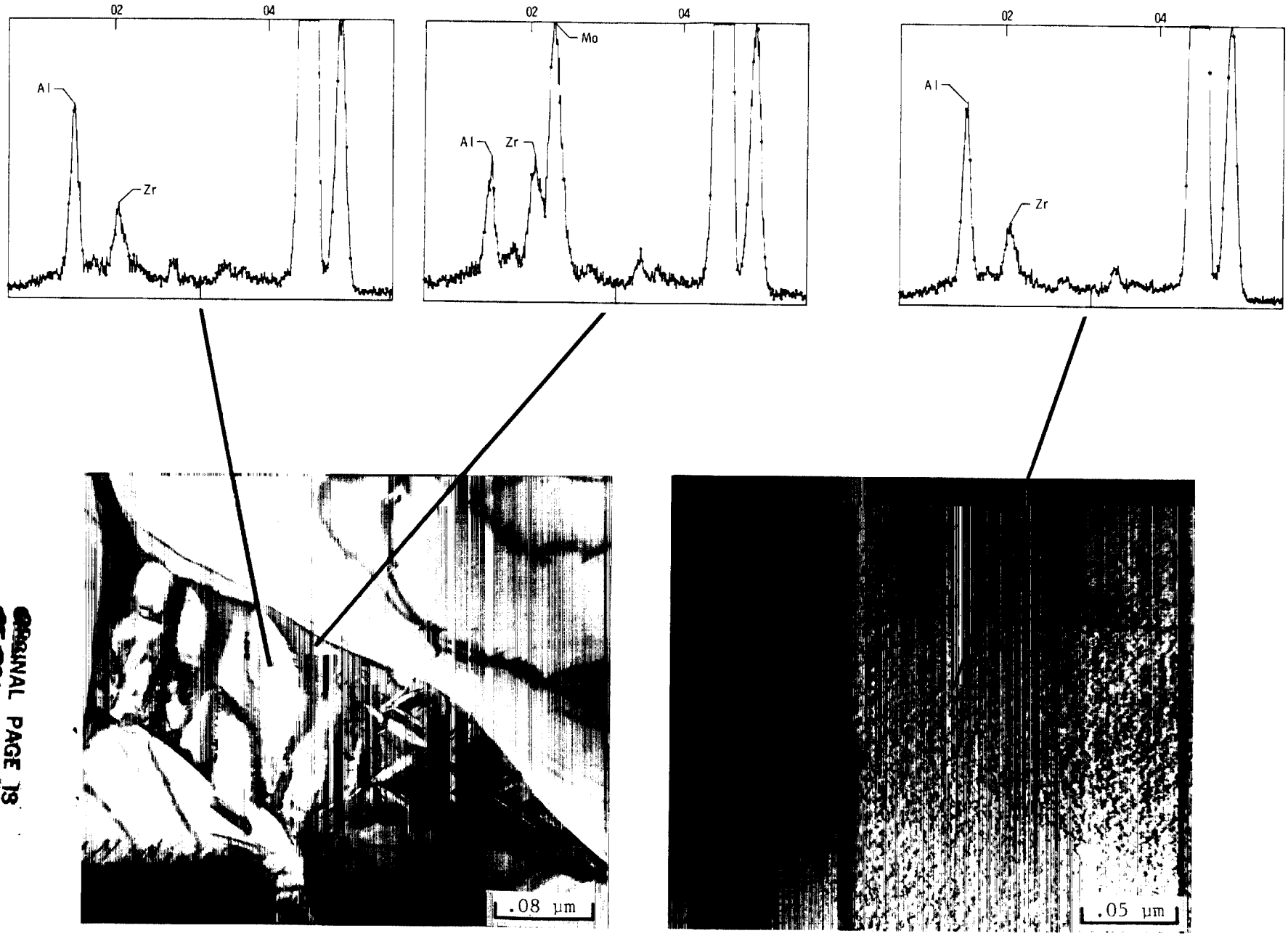

L-87-549

Figure 21. TEM micrographs and chemistries of 100-percent SPF-strained Ti-6242 sheet.

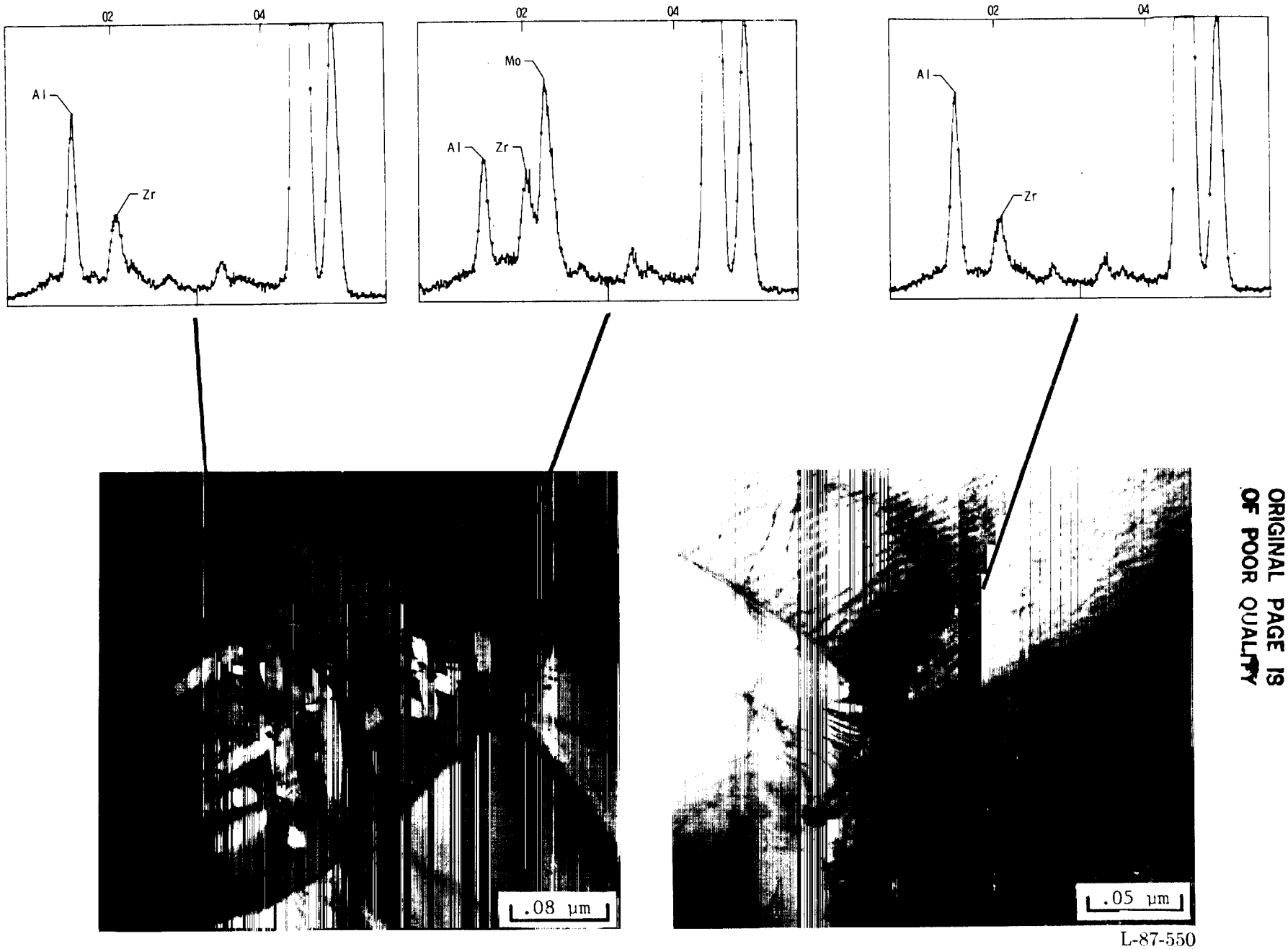

L-87-550

Figure 22. TEM micrographs and chemistries of Ti-6242 duplex annealed after 100-percent SPF strain.

NASA
National Aeronautics and Space Administration

Report Documentation Page

1. Report No.	2. Government Accession No.	3. Recipient's Catalog No.
NASA TP-2674		

4. Title and Subtitle	5. Report Date
Material Characterization of Superplastically Formed Titanium (Ti-6Al-2Sn-4Zr-2Mo) Sheet	May 1987
	6. Performing Organization Code
7. Author(s)	8. Performing Organization Report No.
William A. Ossa and Dick M. Royster	L-16115
9. Performing Organization Name and Address	10. Work Unit No.
NASA Langley Research Center Hampton, VA 23665-5225	505-43-43-06
	11. Contract or Grant No.
12. Sponsoring Agency Name and Address	13. Type of Report and Period Covered
National Aeronautics and Space Administration Washington, DC 20546-0001	Technical Paper
	14. Sponsoring Agency Code

15. Supplementary Notes

William A. Ossa: PRC Kentron, Inc., Hampton, Virginia.
Dick M. Royster: Langley Research Center, Hampton, Virginia.

16. Abstract

The aerospace industry has focused considerable interest on the near-alpha titanium alloy Ti-6Al-2Sn-4Zr-2Mo (Ti-6242) because of both its high-temperature properties and its superplastic forming (SPF) capabilities. This paper describes current research to characterize selected mechanical properties of Ti-6242 sheet in the SPF-strained condition, both with and without heat treatment, and compares the results with those obtained on as-received material. Tensile and creep tests were conducted, and metallographic analysis was performed to show the effect of 100 to 700 percent SPF strain on titanium properties. Analysis shows that as a result of SPF processing, both tensile and yield strengths, as well as elongation, are moderately reduced. Creep tests at 800°F and 1000°F show that the SPF processed material displays superior creep resistance compared with the as-received material. A post-SPF duplex-anneal heat treatment had no beneficial effect on tensile and creep properties.

17. Key Words (Suggested by Authors(s))	18. Distribution Statement
Ti-6242 Superplastic forming Creep Tensile Microstructure Duplex anneal	Unclassified—Unlimited Subject Category 26

19. Security Classif.(of this report)	20. Security Classif.(of this page)	21. No. of Pages	22. Price
Unclassified	Unclassified	37	A03

NASA-Langley, 1987